

THE SILESIAN UNIVERSITY OF TECHNOLOGY
FACULTY OF CHEMISTRY
DEPARTMENT OF ORGANIC CHEMISTRY, BIOORGANIC
CHEMISTRY AND BIOTECHNOLOGY

Ali Maruf, M.Eng.

DOCTORAL DISSERTATION

The collection of published and thematically related articles

Trehalose releasing nanogels for autophagy stimulation

Supervisor: prof. dr hab. inż. Ilona Wandzik

Supporting supervisor: dr inż. Małgorzata Milewska

Gliwice 2024

Funding and Institutional Acknowledgements



Research was financed under the PRELUDIUM BIS 1 project (2019/35/O/ST5/02746) from The National Science Centre (NCN), Poland; project title “Trehalose releasing nanogels for autophagy stimulation.”



Six-month research internship at The University of Helsinki, Finland was financed by The Polish National Agency for Academic Exchange (NAWA), which provided the mobility scholarships under NAWA Preludium Bis 1 Doctoral Internship Program (PPN/STA/2021/1/00053/U/DRAFT/00001).



Two-week internship at The University of Coimbra, Portugal was financed by PROM Program (POWR.03.03.00-IP.08-00-P13/18).

Three-month internship at The University of Groningen, The Netherlands was partly financed by The Silesian University of Technology as the mobility scholarship for the best PhD students of 2023/2024 academic year under the implementation of The Excellence Initiative – Research University program (IDUB, 2020–2026).

Personal Acknowledgements

I still find it hard to believe that my four years of PhD study are almost over. Time flies when we enjoy something, and I owe huge thanks to everyone who supported me along the way.

First and foremost, I would like to thank **Iłona** as my supervisor and **Gosia** as supporting supervisor. **Iłona**, It is hard for me to put into words how fortunate I am to have you as my PhD supervisor. You are always there for me when I need advice, guidance, direction, ideas, support, or anything else related to my study, living in Poland, or traveling around Europe. I appreciate all your help and patience. Thank you for believing me. **Gosia**, without your tremendous assistance, my PhD would not have been possible to complete. I appreciate all your insightful suggestions and thoughts. It has been a great pleasure to learn a lot from you and to work with you.

I would also like to thank the rest of the Sweet team and all people in the Biotechnology Center, especially in the ground floor, for making my time in the lab so memorable and for all of their help and support over the past four years.

Next, I would like to thank our previous and present research collaborators. **Dr. Olga Borges** from The University of Coimbra, Portugal; **Dr. Máté Varga** from the Department of Genetics, Eötvös Loránd University (ELTE), Hungary; **Prof. Wei Wu** from Chongqing University, China; **Prof. Mikko Airavaara** and **Dr. Andrii Domanskyi** from The University of Helsinki, Finland; and **Prof. Anna Salvati** from The University of Groningen, The Netherlands.

Finally, my heartfelt thanks go to my family in Indonesia. To my mom, my sister, my wife, and my daughter **Nana**—your unconditional support has been my strength. I love you and I miss you dear all. I dedicate this dissertation to each of you. Living in Poland without your presence has been difficult, but I promise that a joyful reunion awaits when I will return to Indonesia, or bring you to Europe for some more years hopefully, so we can live together happily once again.

Ali

Gliwice, 15 April 2024

“Wherever you wanna go, sky is the limit”

Nicole Kidman, Roar 2022

[If you set your mind to something, everything is possible. There is no limit—
the sky is the limit.]

Streszczenie

Autofagia to zależny od lizosomów proces polegający na kontrolowanym rozkładzie niepotrzebnych i uszkodzonych składników wewnątrzkomórkowych. Wiele zaburzeń u ludzi jest silnie skorelowanych z nieprawidłowym funkcjonowaniem autofagii. Liczne badania wykazały, że naturalnie występujący disacharyd - trehaloza, wykazuje zdolność do indukowania autofagii. Niestety, ze względu na wysoką hydrofilowość oraz podatność na hydrolizę enzymatyczną trehaloza charakteryzuje się niską biodostępnością. Alternatywą dla wolnej trehalozy, mającą zwiększać jej skuteczność, mogą być nanonośniki zawierające chemicznie skoniugowaną lub fizycznie spułapowaną trehalozę.

Niniejszą rozprawę doktorską stanowi cykl artykułów dotyczących syntezy, charakterystyki oraz zastosowania nanożeli uwalniających trehalozę jako potencjalnych nośników trehalozy do stymulacji autofagii. W pierwszej kolejności opracowano sposób syntezy nanożeli za pomocą fotoinicjowanej polimeryzacji wolnorodnikowej prowadzonej w odwróconej miniemulsji. Trehaloza została kowalencyjnie skoniugowana z siecią polimerową nanożeli poprzez wiązanie estrowe, którego specyficzna lokalizacja umożliwia hydrolizę w warunkach fizjologicznych, w wyniku czego uwalnia się trehaloza. Na uwalnianie trehalozy duży wpływ ma skład nanożeli, ładunek sieci i pH środowiska. Uwalnianie nie jest natomiast zależne od stężenia nanożeli. Nanożele uwalniające trehalozę mają kulisty kształt, średnicę hydrodynamiczną w zakresie od 57 do 266 nm oraz dodatni lub ujemny potencjał zeta zależny od ładunku wbudowanych ugrupowań jonowych. Najlepsze z opracowanych nanożeli charakteryzują się wysoką zawartością trehalozy (~50% w/w), są stabilne koloidalnie, dobrze wchłaniane przez komórki, nie są cytotoksyczne, oraz nie powodują hemolizy. Badania biologiczne potwierdziły, że opracowane nanożele działają stymulująco na proces autofagii. Pierwsze badanie wykazało, że nanożele mogą stymulować autofagię *in vivo* w dwóch organizmach modelowych: transgenicznym danio przęgowym oraz larwach *Drosophila*. W drugim badaniu wykazano, że stymulacja autofagii przez nanożele korzystnie wpływa na redukcję blaszki miażdżycowej w mysim modelu miażdżycy. Opracowane nanożele stanowią nowy rodzaj nanonośników zawierających trehalozę i można je uznać za znaczące osiągnięcie w tej dziedzinie, ponieważ dotychczas nie opracowano sposobu kowalencyjnego związania trehalozy z nanonośnikiem, tak by umożliwić jej późniejsze uwalnianie w środowisku o pH 7.4. Biorąc pod uwagę obiecujące wyniki badań nad stymulacją autofagii, opracowane nanożele mogą przyczynić się do dalszego rozwoju skutecznej strategii dostarczania trehalozy w leczeniu chorób związanych z zaburzeniami autofagii.

Abstract

Autophagy is a lysosomal-dependent, cellular recycling process responsible for degradation of unnecessary and damaged intracellular components. Many human disorders are strongly correlated with the malfunctioning of autophagy. Trehalose is a naturally occurring disaccharide that has gained considerable attention, thanks to numerous studies, which demonstrated its ability to induce autophagy. Unfortunately, trehalose has low bioavailability due to its high hydrophilicity and susceptibility to enzymatic hydrolysis. To enhance the efficacy of trehalose, trehalose-bearing nanocarriers, in which trehalose is incorporated either by chemical conjugation or physical entrapment, have emerged as an alternative option to free trehalose.

This doctoral dissertation is a collection of published articles focused on the synthesis, characterization, and the application of trehalose-releasing nanogels as potential trehalose carriers for autophagy stimulation. First, the synthesis of nanogel *via* photoinitiated free radical polymerization in inverse miniemulsion was optimized. Trehalose was covalently conjugated to the polymer network *via* an ester bond, of which the specific location enabled its cleavage under physiological conditions resulting in trehalose release. Trehalose release appeared to be highly influenced by the composition of nanogels, the ester part through which trehalose is incorporated, network charge, and pH of environment, but it was not concentration-dependent. Trehalose-releasing nanogels were characterized by spherical shape with hydrodynamic diameter ranging from 57 to 266 nm and positive or negative zeta potential depending on the charge of the incorporated ionic moieties. The best of the developed nanogels had high content of conjugated trehalose (~50% w/w), were colloiddally stable in serum-enriched media, non-cytotoxic to human umbilical vein endothelial cells, well uptaken by cells, and non-hemolytic to human red blood cells.

Two independent biological studies confirmed the autophagy stimulation effects of trehalose-containing nanogels. First, nanogels were capable to induce autophagy in transgenic zebrafish and *Drosophila* larvae. Second, they demonstrated the therapeutic effects of autophagy stimulation in promoting lipid efflux and plaque reduction in a mouse model of atherosclerosis. The developed nanogels represent a novel type of trehalose-bearing nanocarriers, and can be considered as a significant achievement in this field, because nanocarriers characterized by covalent conjugation of trehalose, which can be sustainably released at pH 7.4 have not been developed so far. Taking into account the promising results from autophagy stimulation studies, the developed nanogels may contribute to the further development of an effective trehalose delivery strategy to overcome impaired autophagy-related disorders.

Table of content

List of abbreviations	7
List of publications	8
1. Research aims and the scope of the study	9
2. Literature background	10
2.1. Nanoparticles for drug delivery	10
2.2. Nanogels as nanocarriers	12
2.3. Trehalose in biomedical applications	13
2.4. Trehalose-containing nanocarriers to target impaired autophagy	15
3. Results	18
3.1. Elaboration of free radical polymerization in inverse miniemulsion for nanogel synthesis	18
3.1.1. Anionic nanogels as doxorubicin carrier	20
3.1.2. Cationic nanogels for miRNA complexation	22
3.2. Trehalose-containing nanogels	24
3.2.1. Synthesis of trehalose monomers	25
3.2.2. Synthesis and physicochemical characterization of nanogels	26
3.2.3. Trehalose release study	34
3.3. Biological studies on trehalose-releasing nanogels	38
3.3.1. Autophagy stimulation in <i>Drosophila</i> and zebrafish larvae	39
3.3.2. Autophagy stimulation for atherosclerosis treatment in mice	41
3.4. Fluorescent labeling of nanogels for imaging in biological studies	43
4. Summary and conclusions	48
5. References	50
6. Academic achievements	57

List of abbreviations

4-AMBA	4-Acrylamidobutanoic acid
AM	Acrylamide
AMPK	AMP-activated protein kinase
AMPTMAC	3-Acrylamidopropyltrimethylammonium chloride
AMT	Adsorptive-mediated transcytosis
ATC	[2-(Acryloyloxy)ethyl]trimethylammonium chloride
BBB	Blood-brain barrier
CBA	<i>N,N'</i> -Bis(acryloyl)cystamine
CEA	2-Carboxyethyl acrylate
CNS	Central nervous system
CTre	Conjugated trehalose
DDS	Drug delivery systems
d_H	Hydrodynamic diameter
DLS	Dynamic light scattering
DMAM	<i>N,N</i> -Dimethylacrylamide
DOX	Doxorubicin
EPR	Enhanced permeability and retention
FRP	Free radical polymerization
GLUT	Glucose transporter
GSH	Glutathione
HUVECs	Human umbilical vein endothelial cells
LC3	Microtubule-associated protein 1A/1B-light chain 3
MBA	<i>N,N'</i> -methylenebisacrylamide
miRNA	MicroRNA
NADPH	Nicotinamide-adenine dinucleotide phosphate
NAFLD	Nonalcoholic fatty liver disease
PEG ₄₀₀ DA	Poly(ethylene glycol) ₄₀₀ diacrylate
SQSTM1/p62	Sequestosome 1
TFEB	Transcription factor EB
TMS	Trimethylsilyl
TreA	Trehalose 6- <i>O</i> -acrylate
TreMA	Trehalose 6- <i>O</i> -methacrylate

List of publications

This Doctoral dissertation consists of the following collection of published and thematically related articles:

- [P1] Maruf A*, Milewska M*, Varga M, Wandzik I*. *Trehalose-Bearing Carriers to Target Impaired Autophagy and Protein Aggregation Diseases*. **J. Med. Chem.** 2023, 66, 15613–15628. DOI: 10.1021/acs.jmedchem.3c01442. (IF₂₀₂₂ = 7.300, MEiN = 200 point, *contributed equally)
- [P2] Maruf A, Milewska M, Lalik A, Wandzik I. *pH and Reduction Dual-Responsive Nanogels as Smart Nanocarriers to Resist Doxorubicin Aggregation*. **Molecules**. 2022, 27, 5983. DOI: 10.3390/molecules27185983. (IF₂₀₂₁ = 4.927, MEiN = 140 point)
- [P3] Maruf A, Milewska M, Lalik A, Student S, Wandzik I. *A Simple Synthesis of Reduction-Responsive Acrylamide-Type Nanogels for miRNA Delivery*. **Molecules**. 2023, 28, 761. DOI: 10.3390/molecules28020761. (IF₂₀₂₂ = 4.600, MEiN = 140 point)
- [P4] Maruf A, Milewska M, Kovács T, Varga M, Vellai T, Lalik A, Student S, Borges O, Wandzik I. *Trehalose-releasing nanogels: A step toward a trehalose delivery vehicle for autophagy stimulation*. **Biomater. Adv.** 2022, 138, 212969. DOI: 10.1016/j.bioadv.2022.212969. (formerly known as **Mater. Sci. Eng. C** with IF₂₀₂₁ = 7.328, MEiN = 140 point)
- [P5] Zhong Y*, Maruf A*, Qu K, Milewska M, Wandzik I, Mou N, Cao Y, Wu W. *Nanogels with covalently bound and releasable trehalose for autophagy stimulation in atherosclerosis*. **J. Nanobiotechnol.** 2023, 21, 472. DOI: 10.1186/s12951-023-02248-9. (IF₂₀₂₂ = 10.200, MEiN = 140 point, *contributed equally)

Total IF = 34.355, Average IF = 6.871, Total MEiN = 760 point

Patent application

Ilona Wandzik, Małgorzata Milewska, Ali Maruf; Sposób otrzymywania nanożeli uwalniających kowalencyjnie związaną trehalozę.

Patent application number: P.438753 , submission date: 16 August 2021, Urząd Patentowy RP, Warszawa, Poland.

1. Research aims and the scope of the study

This doctoral dissertation is a collection of five published articles: one literature review presenting the current state of the research in the field of trehalose carriers targeting impaired autophagy, and four research articles focused on the synthesis, characterization, and the application of trehalose-releasing nanogels as potential trehalose carriers for autophagy stimulation. The collection of articles is supplemented with patent application. The primary aim of the work was to address the issue of poor trehalose bioavailability by developing covalent, yet hydrolytically-labile (releasable) incorporation of trehalose into nanogels to create nanogels that can release trehalose at systemic pH. Another aim was to evaluate capability of the developed trehalose-releasing nanogels to stimulate autophagy.

The scope of the study included:

- Elaboration of the synthesis of nanogels *via* photoinitiated free radical polymerization in inverse miniemulsion to establish optimal conditions for synthesis of trehalose-releasing nanogels.
- Study on the influence of the composition of trehalose-releasing nanogels on their physicochemical characteristics. The physicochemical characterization included: confirmation of covalent trehalose incorporation (by ^1H NMR), imaging (by cryoTEM), determination of trehalose content (by enzymatic assay), determination of hydrodynamic diameter (d_H) and zeta (ζ)-potential (by DLS and ELS, respectively), and evaluation of colloidal stability in selected biological media (by turbidimetry and DLS).
- Study on trehalose release from nanogels focusing on how it is influenced by nanogels composition as well as nanogels concentration and solution pH. The following compositional aspects were considered: content and structure of acrylamide-type units, type of trehalose ester and type of ionic functionalization.
- Fluorescent labeling of nanogels for bioimaging purposes by two different approaches. The first approach involved introducing the fluorescent moiety during polymerization, while the second approach involved incorporating it after polymerization.
- Evaluation of cytocompatibility and hemocompatibility of trehalose-releasing nanogels.
- Investigation on autophagy inducing potential of trehalose-releasing nanogels in *in vitro* and *in vivo* study in collaboration with Dr. Máté Varga's group from Eötvös Loránd University (ELTE), Hungary and Prof. Wei Wu's group from Chongqing University, China.

2. Literature background

2.1. Nanoparticles for drug delivery

In the past fifty years, nanoparticles have been a subject of extensive study as potential drug delivery systems (DDS) and diagnostic tools [1], [2], [3]. Unique characteristics of colloidal nanoparticles demonstrate potential use as nanocarriers to transport drugs and facilitate a controlled drug release at the site of action [1], [3], [4]. Nanocarriers could offer improved solubility for hydrophobic drugs/active compounds [5] as well as improved bioavailability and pharmacokinetics profile in comparison to free therapeutics [1], [6].

Nanocarriers are designed to address the challenges of free therapeutic delivery, particularly in maneuvering various biological barriers, including systemic, microenvironmental, and cellular barriers [1], [3]. The ideal size of nanocarriers is usually between 50 to 100 nm, in order to prevent accumulation and clearance by the liver, spleen, or kidneys [7].

In recent years, the application of DDS using nanocarriers has been explored in pre-clinical studies for treatments of major human diseases (*e.g.*, cancers, cardiovascular diseases, diabetes, neurodegenerative diseases, and autoimmune diseases) [1], [2], [8]. Nanocarriers can be administered *via* many different routes, but parenteral administration *via* intravenous injection is the most extensively studied method [9].

Several significant advancements mark the evolution of nanocarrier development. Following the discovery of liposomes in 1964, a number of significant advances have emerged including the first study of controlled release polymeric systems in 1978, the introduction of targeted liposomes in 1980, the identification of the enhanced permeability and retention (EPR) effect in 1986, and the development of long circulating nanocarriers with poly(ethylene glycol) (PEG) coating in 1994 [10]. The first drug-loaded nanocarrier to receive FDA approval was Doxil (doxorubicin (DOX)-encapsulated liposome), which was approved in 1995 [1]. Afterwards, numerous nanocarrier systems underwent clinical trials and received FDA approvals, including lipid-based nanocarriers (*e.g.*, DaunoXome, AmBisome, and Visudyne), polymeric nanocarriers (*e.g.*, Copaxone, PegIntron, and Eligard), and inorganic nanocarriers (*e.g.*, DexFerrum, Ferrlecit, and Venofer) [1]. However, despite extensive research on the development of nanocarriers, their presence in the market remains limited.

Generally, nanocarriers can be classified into organic, inorganic, and hybrid nanocarriers [1]. Examples of organic nanocarriers include: solid lipid nanoparticles, liposomes, dendrimers, polymeric nanoparticles, and micelles. Inorganic nanocarriers include: carbon nanotubes, metal nanoparticles, quantum dots, and mesoporous silica nanoparticles. In turn, an example of hybrid

nanocarriers may be inorganic nanoparticles coated with a polymer [1], [2], [8]. On top of that, polymeric nanocarriers are considered as one of the most widely studied carriers for DDS and can be classified into either synthetic or natural [11], [12]. The synthetic one offers controllable physicochemical properties (size, shape, and mechanical properties), tunable degradation, high reproducibility, and easy surface functionalization, but it can be more cytotoxic compared to the natural one and require complex and multi-step synthesis procedures [11], [12]. Meanwhile, the natural one offers good biocompatibility, abundant resources in nature, and intrinsic bioactivity, but it can have high batch-to-batch variability and limited functional groups for surface modification [11], [12].

Nanocarriers surface can be functionalized with different targeting ligands, imaging molecules, protein/peptides, and specific polymers (*e.g.*, PEG) to improve their properties including specific targeting, diagnostic, and stealthy properties [13], [14]. Other functionalization includes the incorporation of stimuli-responsive moieties/crosslinkers/particles that are responsive to endogenous or exogenous stimuli (*e.g.*, pH, enzymes, glutathione (GSH), light, magnetic field, and ultrasound), which create smart nanocarrier systems [14], [15].

Generally, there are three possible ways of loading drugs into nanocarriers. The first approach involves physical entrapment of drugs within nanocarriers [16], [17]. For instance, nanoprecipitation and emulsion solvent evaporation are two popular methods for physical loading [18], [19]. The second approach is complexation between the drug molecules and specific components of nanocarriers. For example, polymer-drug complex *via* electrostatic interaction between negatively charged drugs and chitosan or polyethyleneimine (PEI) or ligand-drug complex *via* specific affinity between drug molecules and ligands/antibodies. The third method involves chemical conjugation of drugs into nanocarriers to form polymer-drug conjugates by incorporating cleavable linkers [20], [21], [22]. The last approach protects drugs more effectively by restricting inactivation or degradation of drugs from certain physiological enzymes and/or preventing premature release of drugs, particularly for hydrophilic drugs that are easily released if encapsulated physically [20], [21], [22]. Controlled release of the payloads in polymer-drug conjugates is usually achievable by incorporating labile-bonds such as acid-labile bonds (*e.g.*, imine, acetal, hydrazone, and to some extent 3-thiopropionate ester) and disulfide bonds as redox-labile bonds [21]. Their cleavage is usually relatively fast and the conjugated drug can be completely released in the range of several hours to a few days. Linkages including esters, amides, and carbamate, which are more stable and rather resistant to hydrolysis under physiologically relevant conditions, are also used for drug conjugation. In these cases, complete release of the drug requires very long time, what is more beneficial for

continuous and prolonged release. Sometimes, their cleavage can be accelerated in the presence of enzymes. In addition to small molecule drugs, proteins and peptides can also be conjugated into polymeric nanocarriers [20].

2.2. Nanogels as nanocarriers

Nanogels, also known as hydrogel nanoparticles, are nanoparticles composed of physically or chemically cross-linked hydrophilic or amphiphilic polymer networks and a large quantity of water [23], [24], [25]. Nanogels have unique properties such as high swelling ability (water entrapment), high drug loading capacity, tunable size, softness, and high stability in biological media or during long-term storage. Other important benefit of nanogels is their ability to encapsulate different types of bioactive substances and drugs and biomacromolecules such as protein or DNA without affecting their gel-like characteristic [25]. Nanogels have been extensively studied in biomedical applications, including their potential use in DDS, wound healing application, as well as tissue engineering and regenerative medicine [25], [26]. More specifically, smart nanogels, *i.e.*, nanogels with responsiveness toward endogenous and/or exogenous stimuli, have currently been studied for drug delivery, gene delivery, bioimaging and biosensing, photodynamic therapy, and photothermal therapy [27].

Generally, nanogels can be synthesized through various methods, including self-assembly of interacting polymers utilizing non-covalent interactions (*e.g.*, *via* hydrogen bonding, electrostatic interactions, hydrophobic interactions, or van der Waals forces), polymerization of hydrophilic monomers, cross-linking of preformed polymers, and template-assisted nanofabrication [23]. Nanogels can be functionalized through two different methods: post-synthetic modifications, which involve chemically modifying nanogels after their synthesis or through pre-synthetic approaches, *e.g.*, synthesizing nanogels by polymerization using monomers containing functional moieties [26], [28].

Nanogels hold significant promise to facilitate the transport of drugs to the central nervous system (CNS) for the treatments of neurodegenerative diseases and brain tumors [29], [30]. In this case, nanogels are designed to cross the blood-brain barrier (BBB) and blood-cerebrospinal fluid barrier (BCSFB) utilizing different functionalization, such as ligand and charge modification as well as magnetic-guided delivery [29], [30]. The size and surface charge of nanogels are two important factors for successful therapeutic delivery to the brain. Nanogels with particle sizes smaller than 100 nm are preferable to cross the BBB [31], [32]. Surface functionalization with middle or high molecular weight ligands, such as insulin or transferrin, can further enhance the delivery efficiency of nanogels to the CNS *via* receptor-mediated

transcytosis, due to the specific interaction with insulin and transferrin receptors on the neuron cell membranes [31], [32]. On the other hand, because the exterior membrane of brain endothelial cells is negatively charged, positively charged nanogels may exploit the adsorptive-mediated transcytosis (AMT) route with greater efficacy than their neutral or negatively charged counterparts [33], [34]. Cargo encapsulation into nanogels can be achieved during or after nanogel synthesis. Small molecule drugs, proteins or peptides, and oligonucleotides are some examples of potential cargos which can be loaded into nanogels and delivered to the CNS [29], [31]. Controlled release of the encapsulated cargos from nanogels generally can be achieved either by diffusion, degradation, ion displacement, pH shift, or external energy (*e.g.*, magnetic field, ultrasound, and light), which can also be applied for CNS delivery [29].

2.3. Trehalose in biomedical applications

Many years ago, people understood that carbohydrates were just a source of energy but then it turns out that some of them play specific roles in biological systems. Trehalose, for instance, is one of the most important disaccharides due to its high stability (resistance to high temperature and hydrolysis) and unique properties, *e.g.*: cryo-protection, protein stabilization, and autophagy induction [35], [36]. Trehalose, however, can be instantly hydrolyzed by trehalase enzyme that is present in various organisms including human. In nature, trehalose can be found in plants, algae, mushrooms, yeasts, and insects, but not in mammals [35], [36]. The chemical structure of trehalose, a non-reducing homodisaccharide composed of two D-glucose units linked at their anomeric positions by an α,α' -1,1'-glycosidic bond, in comparison to other popular disaccharides, is shown in **Figure 1**.

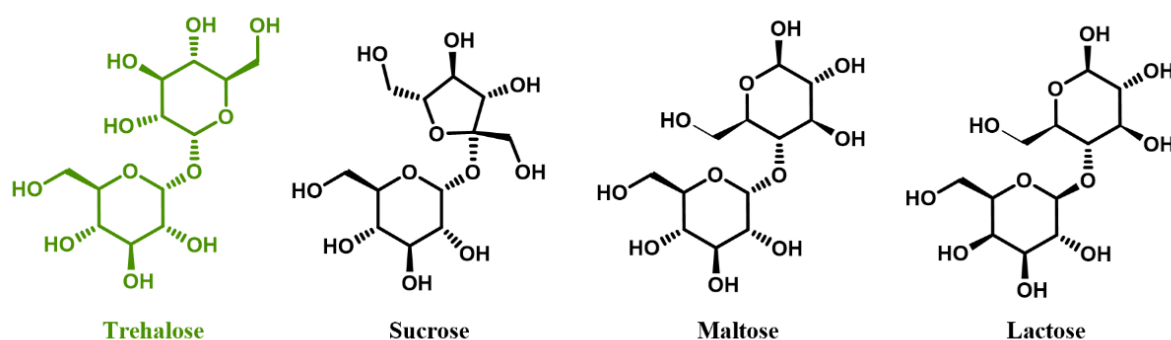


Figure 1. Chemical structure of trehalose in comparison to other disaccharides such as sucrose, maltose, and lactose.

Nowadays, the enzymatic technology has been used for mass production of trehalose using enzymes isolated from bacteria, namely maltooligosyltrehalose synthase and

maltooligosyltrehalose trehalohydrolase, together with α -amylase to break down maltodextrin, for instance from cassava starch, and yield trehalose in large quantities [37].

Trehalose has wide-ranging applications throughout every-day life and healthcare [38]. First, trehalose is widely used as a stabilizing agent in the food industry, particularly to prevent food products against extreme heat during drying process that can reduce the nutrition value, original flavor, and aroma. It is also a popular food additive that is usually used as a sweetener and bulking agent. Second, trehalose finds application in cosmetics, particularly skincare, where it serves as a moisturizing agent due to its ability to bind with water molecules. In addition to its hydrating effects, trehalose acts as a strong antioxidant and protects the skin. Next, trehalose has been used in cryopreservation of human cells, thanks to its ability to prevent ice crystal formation that can damage cell membranes during storage in sub-zero temperature. Furthermore, trehalose is used as a protein stabilizer in a variety of settings, including the biotechnology, pharmaceutical, and medical fields [38]. Some examples of commercially available pharmaceutical products that use trehalose are Thealoz® Duo (Thea Pharma), Advate® (Baxter), Avastin® (Genentech), Lucentis® (Genentech), and Herceptin® (Genentech).

On top of that, autophagy induction property of trehalose and its application in disease treatments is the most promising and interesting topic to study [39], [40], [41]. Autophagy is a cellular recycling process that degrades cytoplasmic components, including damaged organelles, protein aggregates, and lipid droplets and recycles them *via* a degradative organelle–lysosome in response to a variety of stress stimuli (*e.g.*, nutrient and energy stress, hypoxia, and pathogen invasion) [42], [43]. This process is important to maintain cells homeostasis, differentiation, and survival. Due to its critical role in cellular processes, the imbalance and dysfunction of autophagy are connected to a number of human disorders, such as neurodegenerative disorders, cardiovascular disease, pulmonary disorders, renal diseases, cancer, autoimmune disorders, and metabolic syndromes [42], [43].

There are currently two main hypotheses explaining how trehalose induces autophagy. The first pathway involves trehalose blocking glucose and fructose transport through glucose transporter (GLUT) family proteins, creating a low adenosine triphosphate (starvation-like) state which consequently activates unc-51-like kinase 1 (ULK1) and AMP-activated protein kinase (AMPK) and then trigger autophagy [39], [44], [45]. The second mechanism involves the activation of transcription factor EB (TFEB) by trehalose, which promotes autophagy by increasing the production of membrane proteins, lysosomal degradation enzymes, and other autophagy-related components [46].

The clinical trials of trehalose for the treatments of diseases related to impaired autophagy and protein aggregation has been summarized in [P1] [47]. There are currently 9 ongoing clinical trials using trehalose administered orally or intravenously for the treatments of type 2 diabetes, Parkinson's disease, Alzheimer's disease, acute coronary syndrome, amyotrophic lateral sclerosis, and spinocerebellar ataxia type 3 according to the data from the Clinical trials database (<https://clinicaltrials.gov>). One major drawback, however, is that to maintain its ability to induce autophagy, trehalose must be administered at extremely high doses due to its hydrophilic nature and susceptibility to enzymatic degradation [40]. The examples are: 100 mM for *in vitro* study and 2–3 g/kg/day (administered parenterally) or 2–4 w/v (administered orally in drinking water) for *in vivo* study. Additionally, a report in Nature, which was published in 2018, showed that dietary trehalose at doses above 10 mM enhances the virulence of epidemic *Clostridium difficile*, making it urgent to reduce trehalose intake [48].

2.4. Trehalose-containing nanocarriers to target impaired autophagy

Nanocarriers containing trehalose, where trehalose is integrated either chemically or physically, are currently being explored as an alternative option to free trehalose to enhance its efficacy for the treatment of impaired autophagy-associated disorders (*e.g.*, neurodegenerative diseases, nonalcoholic fatty liver disease (NAFLD) and type 2 diabetes, cancer, and atherosclerosis), which has been reviewed in [P1, Table 2 on page 5] [47]. The field is relatively new, with reports mostly published after 2017, leaving many unknowns, limitations, and challenges to be addressed.

A total of 8 studies on trehalose-bearing carriers to stimulate autophagy have been published recently, which include nanocarriers with physically entrapped trehalose (*e.g.*, mesoporous silica nanoparticles and β -cyclodextrin-based nanoassemblies) [49], [50] and nanocarriers with chemically bound trehalose (*e.g.*, nanoassemblies [51], [52], [53], [54] and solid-lipid nanoparticles [55] and glycopolymers [56]). The chemical conjugation of trehalose can be either labile or permanent. The first approach relies on covalent bond which can be cleaved under biologically relevant conditions triggering trehalose release. On the other hand, the second strategy implies trehalose being permanently bound to the carrier, making it non-releasable. In this scenario, “poly-(trehalose)” species, which are composed of several copies of trehalose in a single macromolecule or nanoparticle, are currently the main subject of investigation.

As the mechanism of actions of trehalose-bearing nanocarriers to induce autophagy has not been explained, we hypothesize that there are four possible mechanisms through which

trehalose-containing nanocarriers can stimulate autophagy (**Figure 2**). First, the carrier enters the cell through endocytosis, releases trehalose in cytosol, and subsequently induces autophagy *via* TFEB. Second, the carrier decorated with pendant and permanently bound trehalose penetrates the cell by the same mechanism but interacts directly with autophagy substrates *via* a multivalent binding interaction and/or causes indirect stimulation of autophagy. Third, the carrier interacts with GLUT in a multivalent manner, which blocks the transporter and trigger a starvation-like response that induces autophagy *via* the AMP-activated protein kinase (AMPK) pathway. Last, trehalose interacts with GLUT after being released from the carrier in the extracellular fluid, resulting in a similar effect.

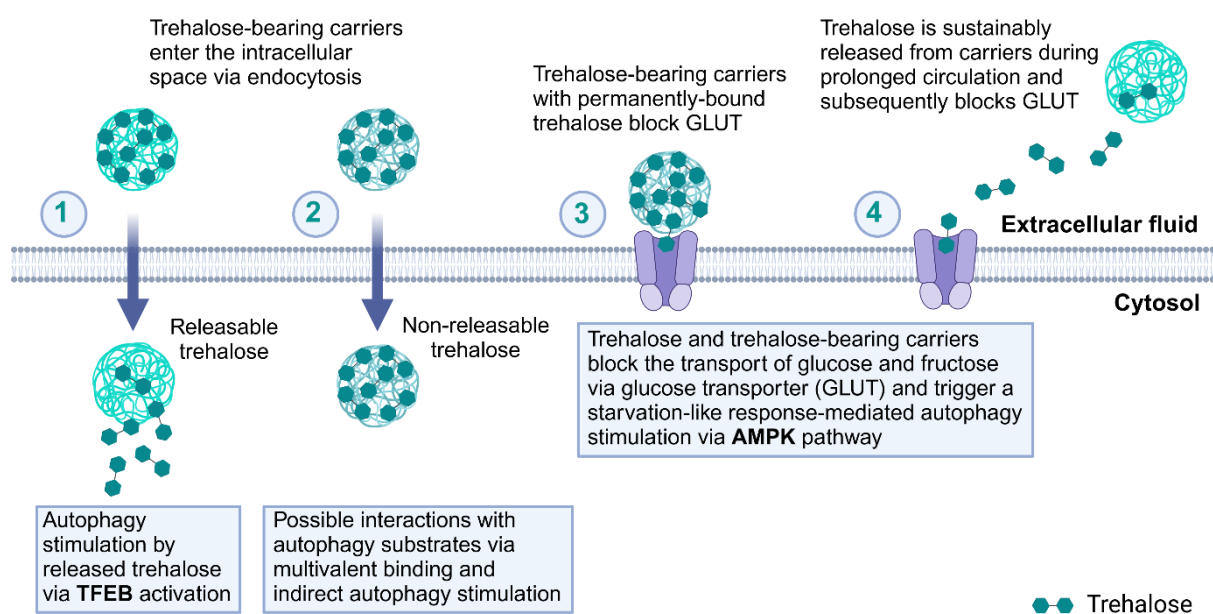


Figure 2. Four possible pathways through which trehalose-bearing carriers can stimulate autophagy. Reproduced with permission from ref. [47]. Copyright 2023 American Chemical Society.

The Seneci group was the first one to investigate the autophagy-stimulating potential of trehalose-bearing carriers by developing nanoassemblies of trehalose-squalene and trehalose-betulinic acid conjugates [54]. However, these nanoassemblies failed to induce autophagy *in vitro*, the most probably due to insufficient free trehalose release. In a subsequent study, two nanoassemblies from trehalose-monosqualene and trehalose-disqualene conjugates containing a biologically labile disulfide bond were fabricated. The disqualene one showed better autophagy induction efficacy than free trehalose and the monosqualene counterpart [51]. The authors hypothesized that this effect is due to the higher permeability of disqualenylated nanoassemblies, which have more hydrophobic cores, through the cellular membrane compared to monosqualenylated nanoassemblies. In the third attempt, trehalose-decorated gold

nanoparticles were prepared through the reduction of gold salt in the presence of thiol-terminated PEG-trehalose conjugate, as trehalose non-releasable nanocarrier [55]. This nanoparticle could successfully induce autophagy *in vitro*, but the mechanism is still unknown. In other group, nanocarriers prepared by either rapid mixing of amphiphilic trehalose–nucleolipid conjugates into solid lipid nanoparticles or encapsulation of the conjugates into PLGA nanoparticles showed enhanced autophagy activity in neuronal cells compared to free trehalose [53]. Other attempt by Chen’s group showed a promising result of enhanced autophagy-mediated cancer cell ferroptosis using trehalose-loaded mSiO₂@MnOx-mPEG nanoparticles [50].

Furthermore, two significant reports have demonstrated the effectiveness of autophagy stimulation by trehalose-bearing carriers to treat atherosclerosis [49], [52]. The first report discusses multiloaded self-assembled nanovesicle systems composed of amphiphilic H9 peptide and hexadecyl phosphorylcholine, which were loaded with trehalose and β-cyclodextrin/oridonin inclusion complex [49]. The second report focuses on constructing nanomotors through the double self-assembly of trehalose conjugates containing four arginine molecules and nanoparticles functionalized by phosphatidylserine, resulting in trehalose-containing nanomotors [52].

In other study two glycopolymers containing 20 or 40 repeating units of 6-*O*-acryloyl-trehalose have been tested for their autophagy-inducing potential in an *in vitro* model of NAFLD [56]. Their polymer backbones were identical, yet they varied in the amount and density of pendant trehalose. While treatment with the glycopolymer containing higher amount of trehalose units in free fatty acid (FFA)-induced lipotoxicity of hepatocytes could significantly induce autophagy, the glycopolymer containing lower amount of trehalose units could only slightly increase the autophagic activity, which was similar to free trehalose.

It is anticipated that considering the increasing number of *in vitro* and *in vivo* studies on trehalose-bearing carriers to stimulate autophagy and treat diseases, the clinical trials of trehalose-containing nanocarrier will likely commence soon, even though no clinical study is presently underway.

3. Results

The research on trehalose-releasing nanogels has started from the elaboration of the optimal polymerization conditions for nanogel synthesis by FRP using inverse miniemulsion technique, what is shortly discussed in the beginning of this chapter. This stage was focused on the synthesis aspects and concerned nanogels without trehalose. As a result of this elaboration cationic and anionic nanogels were developed, which were then studied as carriers for model therapeutics: anionic nanogels for doxorubicin encapsulation ([P2] [57]) and cationic nanogels for miRNA complexation ([P3] [58]). Further discussion in this chapter concerns trehalose-containing nanogels, which were developed based on the elaborated synthesis procedure, and starts from the synthesis of trehalose monomers. The basis of trehalose release from nanogels and rationales for monomers selection are shortly described. The influence of the composition of nanogels on their physicochemical characteristics and trehalose release is thoroughly investigated in ([P4] [59] and [P5] [60]). The main goals concerning the characteristics of trehalose-containing nanogels were to create nanogels with high content of conjugated trehalose, which can be sustainably released at pH 7.4 and which are characterized by high colloidal stability in serum-enriched cell media, hemocompatibility, and lack of cytotoxicity. The biological studies on selected trehalose-releasing nanogels are further discussed, particularly their ability to induce autophagy in transgenic zebrafish and *Drosophila* larvae ([P4] [59]) as well as their potential therapeutic applications to treat atherosclerosis ([P5] [60]). Finally, discussion on two different attempts to label nanogels with fluorescent dyes which have been used for fluorescent imaging in biological studies (in publications [P3] [58], [P4] [59], and [P5] [60]) is provided.

3.1. Elaboration of free radical polymerization in inverse miniemulsion for nanogel synthesis

Nanogels were synthesized *via* photoinitiated free radical polymerization (FRP), involving an inverse miniemulsion method (**Figure 3A**). In this “inverse” setting, water-soluble monomers are dissolved in an aqueous phase, which is dispersed in continuous organic phase, creating a water-in-oil (w/o) emulsion [61], [62], [63]. Generally, miniemulsion can be obtained by high shear force, such as using ultrasonication or high-pressure homogenization. The polymerization occurs in the miniemulsion droplets to afford polymeric nanoparticles with nanoparticle diameter within the diameter range of the droplets, which are generally about 50–500 nm. Herein, the organic phase consisted of cyclohexane and Span 80 as emulsifier, while the

aqueous phase was composed of phosphate buffer, monomers (non-ionic and ionic), crosslinker, photoinitiator and NaCl as osmotic pressure agent. The presence of ionic monomer was important to provide further colloidal stability of nanogels through electrostatic repulsion. Key parameters in nanogel synthesis, which were optimized included: light irradiation wavelength, irradiation direction (bottom-up or top-down), irradiation time, initiator concentration, stirring condition, aqueous to organic phase (w/o) ratio, and monomer concentration in aqueous phase.

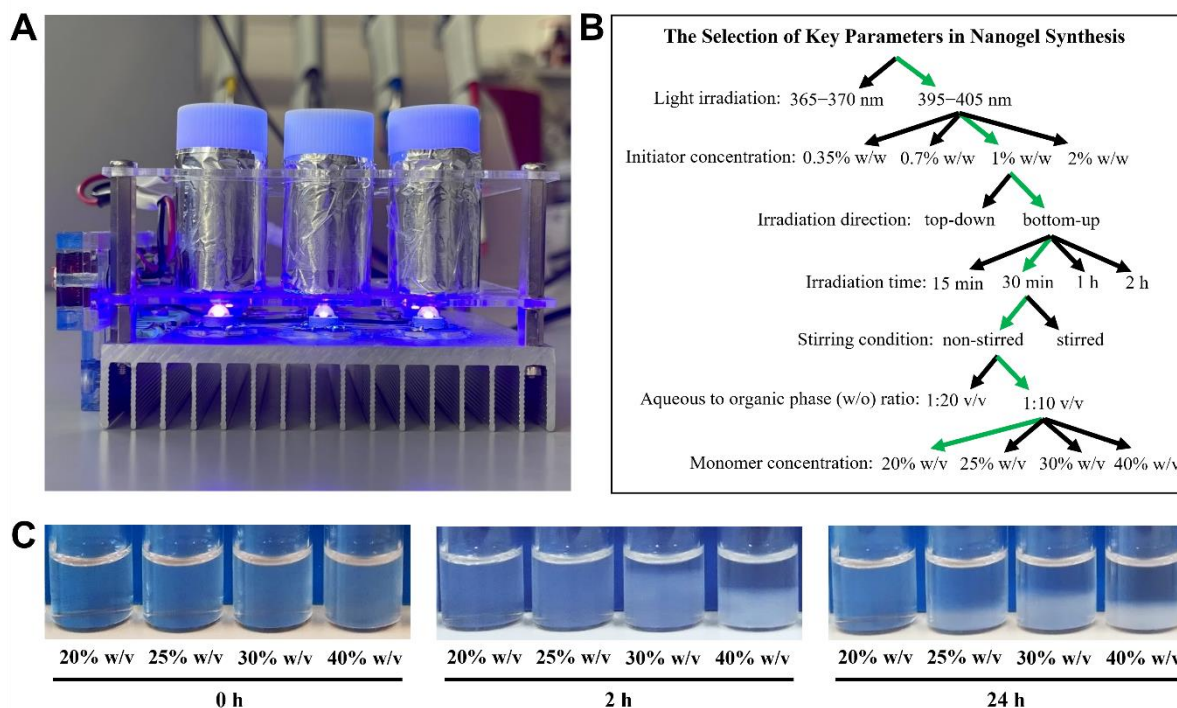


Figure 3. (A) Equipment for the synthesis of nanogels by photoinitiated FRP in inverse miniemulsion using LED (395-405 nm). Vials containing miniemulsion were wrapped with aluminium foils and then exposed to light irradiation from the bottom of the vials. (B) Optimization of nanogel synthesis by photoinitiated FRP in inverse miniemulsion. Green arrows indicate the selected polymerization conditions for the optimized synthesis procedure after carefully evaluating nanogel properties. (C) Visual appearance of colloidal stability of nanogels synthesized with different monomer concentrations in aqueous phase (20, 25, 30, and 40% w/v). Nanogels were dispersed in PBS (pH 7.4) and left for 24 h (nanogel concentration: 1.0 mg/mL).

The optimal parameters were selected considering three following factors: yield, d_H , and colloidal stability in PBS. For example, when selecting stirring condition, low speed stirring (350 rpm) resulted in a bigger size (double) of the obtained nanogels compared to that of polymerization without stirring. Meanwhile, during the reaction carried out with high-speed stirring (>1000 rpm), no polymerization products were formed. Therefore, polymerization reaction was carried out without stirring. In the end of the optimization, reducing the monomer concentrations in aqueous phase from 40% to 20% has been found to greatly improve the colloidal stability of nanogels in biological media (**Figure 3C**). Finally, the selected

polymerization conditions included: bottom-up and 30 min of 395–405 nm light irradiation, 1% w/w LAP initiator, polymerization without stirring, 1:10 v/v of w/o emulsion, and 20% w/v monomer concentration in aqueous phase (**Figure 3B**). The optimization stage resulted in the preparation of anionic and cationic nanogels, which were then studied as nanocarriers for model ionic therapeutics: DOX and miRNA, respectively, and are discussed in chapter 3.1.1 and 3.1.2.

3.1.1. Anionic nanogels as doxorubicin carrier

Doxorubicin (DOX) hydrochloride is one of the most potent chemotherapeutic drugs to treat a wide range of malignancies. However, free DOX has low bioavailability, causes cardiotoxicity, and tends to aggregate into fibril-like structures under physiological conditions [64]. To address these issues, in the first work [**P2**] [57], anionic pH/reduction-responsive, degradable nanogels were synthesized using *N,N*-dimethylacrylamide (DMAM) as the main monomer, 2-carboxyethyl acrylate (CEA) as the ionic monomer, and *N,N'*-bis(acryloyl)cystamine (CBA) as the redox-responsive crosslinker (**Figure 4A**). The obtained nanogels (NG-CBA) were used to encapsulate free DOX *via* electrostatic interactions with the oppositely charged carboxylate moieties from CEA units, with the aim to improve its solubility, prevent DOX aggregation, and control the release of DOX.

While GSH levels in blood plasma are only in micromolar concentrations (2–20 μ M), they can reach millimolar concentrations (2–10 mM) in cytoplasmic cancer environments [65]. Moreover, the pH of the tumor tissue (pH 6.4–7.0) is lower than that of healthy tissues (pH 7.2–7.5) [66]. Therefore, it is expected that DOX release from NG-CBA can be enhanced in two ways. First as a result of protonation of carboxylate moieties at lower pH and weakening of electrostatic interactions. And second, due to the cleavage of disulfide crosslinker in more reductive environment causing nanogels disintegration (**Figure 4A**). In addition, non-degradable nanogels were also synthesized by replacing CBA with *N,N'*-methylenebisacrylamide (MBA) at the equimolar ratio for comparative study.

In general, anionic NG-CBA had average d_H of ~90 nm (PdI = 0.30) and negative ζ -potential of -23.6 mV and were capable to encapsulate DOX with high drug loading capacity (DLC) of up to ~28% w/w [**P2**, *Table 1 on page 4*] [57]. TEM analysis confirmed nanogels degradability in reductive environment [**P2**, *Figure 1 on page 3*] [57]. Nanogels could prevent DOX from aggregating in biological media up to DOX concentrations of ~160 μ g/mL, whereas free DOX was only stable at concentrations lower than 40 μ g/mL [**P2**, *Figure 2 on page 6*] [57]. The visual difference in solubility in biological media between free DOX and that encapsulated in NG-CBA/DOX-1 can be seen in **Figure 4C**.

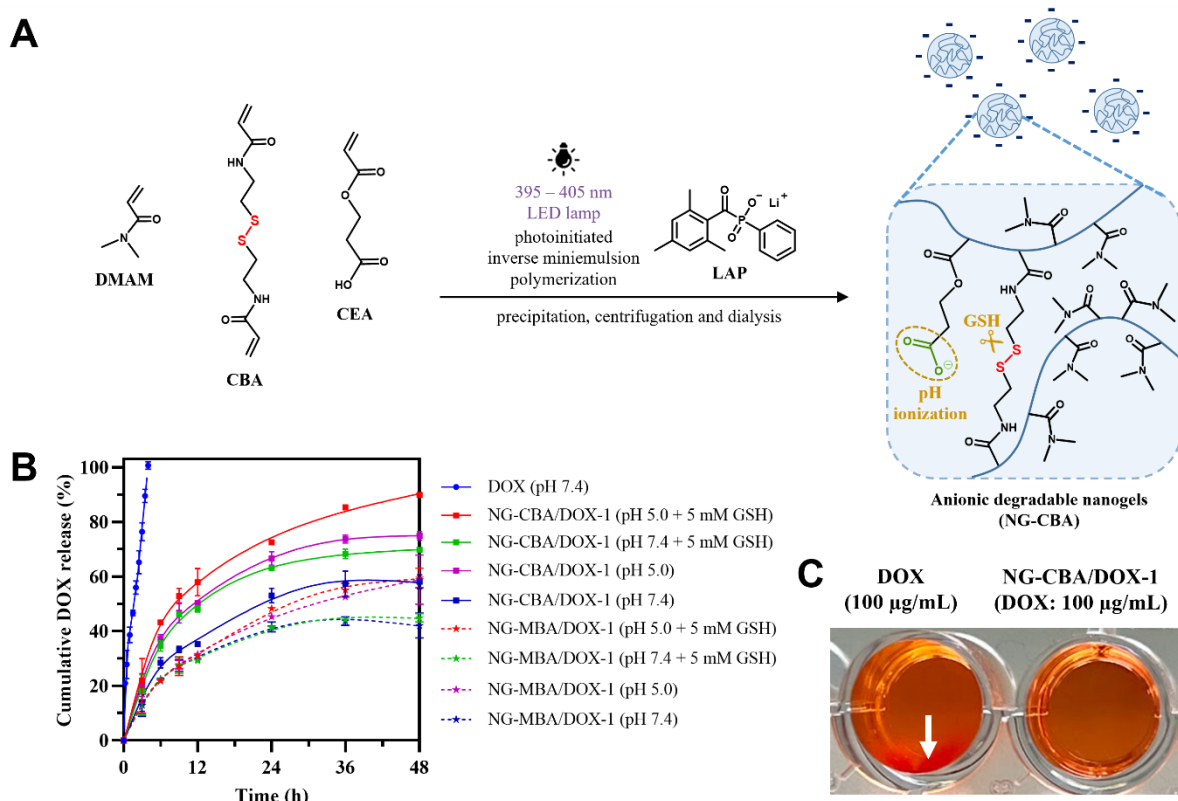


Figure 4. (A) Scheme of the synthesis of anionic, pH/reduction-responsive, degradable nanogels. (B) DOX release profile from NG-CBA/DOX-1 nanogels (squares and solid lines) and NG-MBA/DOX-1 nanogels (stars and dotted lines) in four solutions: GSH (0 and 5 mM) in PBS (pH 7.4 and 5.0) at 37 °C. The data were presented as mean \pm SD ($n = 4$). (C) Visual appearance of DOX (100 $\mu\text{g/mL}$) and NG-CBA/DOX-1 nanogel containing 100 $\mu\text{g/mL}$ of DOX in PBS (pH 7.4) after 1 day at 37 °C. The white arrow indicates DOX aggregates. Adapted with permission from ref. [57] under the terms of the CC BY 4.0 license. Copyright 2022 The Authors, published by Multidisciplinary Digital Publishing Institute.

Furthermore, NG-CBA/DOX-1 showed enhanced DOX release rates at lower pH (*i.e.*, pH 5.0) and in a reducing environment (5 mM GSH) as a result of protonation of carboxylate groups in polymer network and weakening of electrostatic interactions as well as the cleavage of the disulfide crosslinker, showing an obvious pH/reduction dual responsive controlled drug release capability (**Figure 4B**). Meanwhile, NG-MBA/DOX-1 only showed pH-responsive but not reduction-responsive DOX release due to the lack of degradation ability of the MBA crosslinker (**Figure 4B**). *In vitro* studies revealed that the bare nanogel was not cytotoxic to HCT 116 colon cancer cells, whereas DOX-containing nanogels were toxic against HCT 116 colon cancer cells with a slightly better efficacy than free DOX [P2, Figure 4 on page 7] [57]. Taken together the conducted study presented straightforward and facile approach to improve DOX solubility and efficacy.

3.1.2. Cationic nanogels for miRNA complexation

MicroRNA (miRNA), a naturally-occurring noncoding RNA characterized by short 18–25 nucleotide sequences, plays a significant role in regulating diverse cellular mechanisms such as proliferation, programmed cell death, carcinogenesis, and tumor metastasis [67], [68]. Currently, extensive research has been conducted on miRNA-based therapies involving both miRNA antagonists and mimics for cancer treatment [69]. However, the delivery of miRNA encounters obstacles, primarily attributed to low cell uptake and possible degradation by extracellular nucleases abundant in blood plasma, leading to their short half-life [69]. The application of nanocarriers to deliver miRNA is expected to solve these classical problems of free miRNA transfection.

In the second work [P3] [58], cationic degradable nanogels (NG-CBA) were developed for miRNA complexation, which were synthesized using DMAM as the main monomer, [2-(acryloyloxy)ethyl]trimethylammonium chloride (ATC) as the ionic monomer, and CBA as the redox-responsive crosslinker (**Figure 5A**). Antisense miRNA oligonucleotide against miR-21 (a-miR21) was encapsulated into NG-CBA by employing electrostatic interaction between positively charged ATC units in NG-CBA and negatively charged phosphate groups in a-miR21. The obtained cationic NG-CBA had average d_H of ~90 nm (PdI = 0.43) and ζ -potential of +27 mV. After complexation with miRNA at different N/P ratios (NG/a-miR21-1: N/P = 10, NG/a-miR21-2: N/P = 5, and NG/a-miR21-3: N/P = 2), there were a notable increase in d_H as well as a significant reduction of ζ -potential as the N/P ratio decreased. These changes in nanogel properties confirmed the successful complexation of miRNA with NG-CBA. For instance, NG/a-miR21-3 as the best nanogel, showed average d_H of ~120 nm (PdI = 0.43) and ζ -potential of +12 mV [P3, Table 1 and Figure 2 on page 4] [58]. Both bare NG and NG/a-miR21-3 at a concentration of 100 $\mu\text{g/mL}$ had excellent colloidal stability in various biological media, including serum-enriched media [P3, Figure 4 on page 5] [58]. miRNA loading capacity (MLC) was dependent on N/P ratio – the lower N/P, the higher MLC. Meanwhile, miRNA loading efficiency (MLE) was always ~100%. At N/P = 2, NG-CBA was capable to encapsulate a-miR21 up to 6.7% w/w [P3, Table 1 and Figure 2 on page 4] [58]. TEM analysis confirmed nanogels degradability in reductive environment [P3, Figure 3 on page 5] [58].

The cleavage of disulfide bonds causing disintegration of the nanogel network in the presence of GSH had only a minor effect on enhancing miRNA release rate. After 24 h, miRNA release from NG/a-miR21-1, 2, and 3 reached 35.0%, 31.6%, and 55.8%; while, in the presence of GSH (5 mM), the release increased to 49.4%, 44.4%, and 67.4%, respectively. A markedly accelerated release of miRNA was observed in the presence of a strong heparin polyanion,

indicating the reversibility of the complexation. No significant difference was observed in miRNA release between acidic (pH 4.5) and neutral conditions (pH 7.4), which was attributed to the lack of a pH-responsive property of the nanogel (Figure 5B, C).

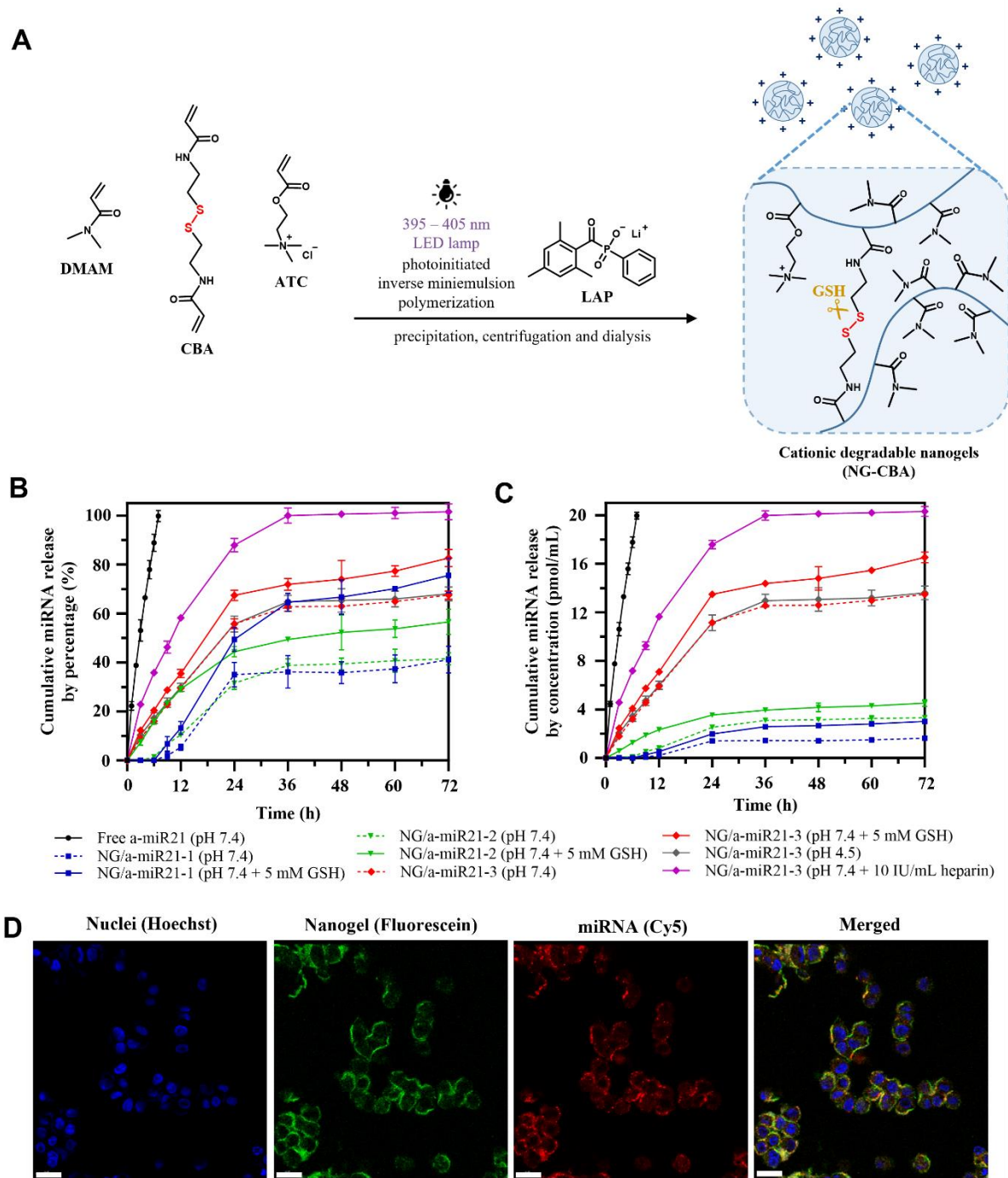


Figure 5. (A) Scheme of the synthesis of cationic degradable nanogels for miRNA complexation. (B, C) miRNA release profile by (B) percentage and (C) concentration from NG/a-miR21-1,2,3 at a nanogel concentration of 100 $\mu\text{g}/\text{mL}$ with or without GSH treatment (5 mM GSH) in PBS (pH 7.4) at 37 $^{\circ}\text{C}$ for 72 h. (D) Cell uptake of FL-NG/Cy5-a-miR21-3 in HCT 116 colon cancer cell line (concentration: 500 $\mu\text{g}/\text{mL}$). Blue color indicates cell nuclei, green color indicates NG-CBA, and red color indicates miRNA. Scale bars = 20 μm . Adapted with permission from ref. [58] under the terms of the CC BY 4.0 license. Copyright 2023 The Authors, published by Multidisciplinary Digital Publishing Institute.

The miRNA-loaded nanogels showed tolerable cytotoxicity and were efficiently uptaken by HCT 116 colon cancer cells [P3, Figure 7 on page 8] [58]. *In vitro* cell uptake study employing fluorescein-labelled nanogels and Cy5-labelled miRNA (FL-NG/Cy5-a-miR21-3) clearly showed that miRNA-loaded nanogels could be uptaken by the cells within 3 h of incubation (Figure 5D).

Summing up, the study present facile method to synthesize miRNA nanocarriers, however further improvements are required. The main issue was very strong complexation of miRNA restricting complete release. It could be improved, *e.g.*, through introduction of groups that have charge switching properties.

3.2. Trehalose-containing nanogels

This and next chapter (3.3.) are based on results from publication [P4] [59] and [P5] [60] and are supplemented in some parts with unpublished results.

Trehalose is a water-soluble and non-charged compound that poses challenges for encapsulation in nanocarriers *via* physical loading due to its tendency for premature release. The effort to covalently attach trehalose to polymers in a way that allows its controlled release at pH 7.4 is quite challenging due to the limited functional groups available, which are only hydroxyl groups. One way to involve hydroxyl group for conjugation is through an ester linkage. The utility of the ester bond to form labile conjugation is limited because hydrolysis rates of esters at physiologically relevant conditions are generally very slow [70]. However specific structural features can boost the hydrolysis rate. For example, McCoy *et al.* demonstrated that the release rate of model antibiotic – nalidixic acid, attached to poly(methyl methacrylate) through an ester linkage can be accelerated and controlled by nucleophilicity, geometry, and steric bulk of neighboring pyridyl or tertiary amine moieties [71]. Very recently, our group have found that in polymeric networks of hydrogels fabricated from acrylamides and acrylates, primary or secondary acrylamide-type units significantly accelerate hydrolysis of ester moiety in acrylate units [72]. Utilizing trehalose mono-/diacrylate, this effect was further exploited to develop bulk trehalose-rich hydrogels capable of sustained trehalose release at pH 7.4 [73]. On this basis, herein we have moved to nanoscale and aimed to develop trehalose-releasing nanogels, which could potentially serve as nanocarriers to deliver trehalose as a potent autophagy inducer. Similarly, trehalose monoacrylate was utilized to ensure labile trehalose incorporation into nanogels. It was combined with various compositions of acrylamide-type comonomers to study the compositional effects on trehalose release rate and physicochemical properties, with the aim to find an optimal nanogel composition for biological study on

autophagy induction. Additionally, influence of the replacement of trehalose monoacrylate by its monomethacrylate analogue on trehalose release was also investigated.

3.2.1. Synthesis of trehalose monomers

The α,α' -trehalose has eight hydroxyl groups, and it is a bit challenging to selectively modify one of them to form monoester. Fortunately, two of these hydroxyls are primary and more reactive than the others. In this regard, our group has successfully developed a multistep regioselective protection/deprotection strategy to synthesize trehalose monoacrylate monomer (6-*O*-acryloyl-trehalose, TreA) with satisfactory yield [73]. Generally, the synthesis procedure includes four steps, and involves trimethylsilyl (TMS) protecting group strategy due to the fact that primary and secondary trimethylsilyl-protected hydroxyl groups have different susceptibilities to methanolysis. In addition, trehalose methacrylate monomer (6-*O*-methacryloyl-trehalose, TreMA) could also be obtained by the same procedure, just by replacing acryloyl chloride with methacryloyl chloride in the third step (**Figure 6**).

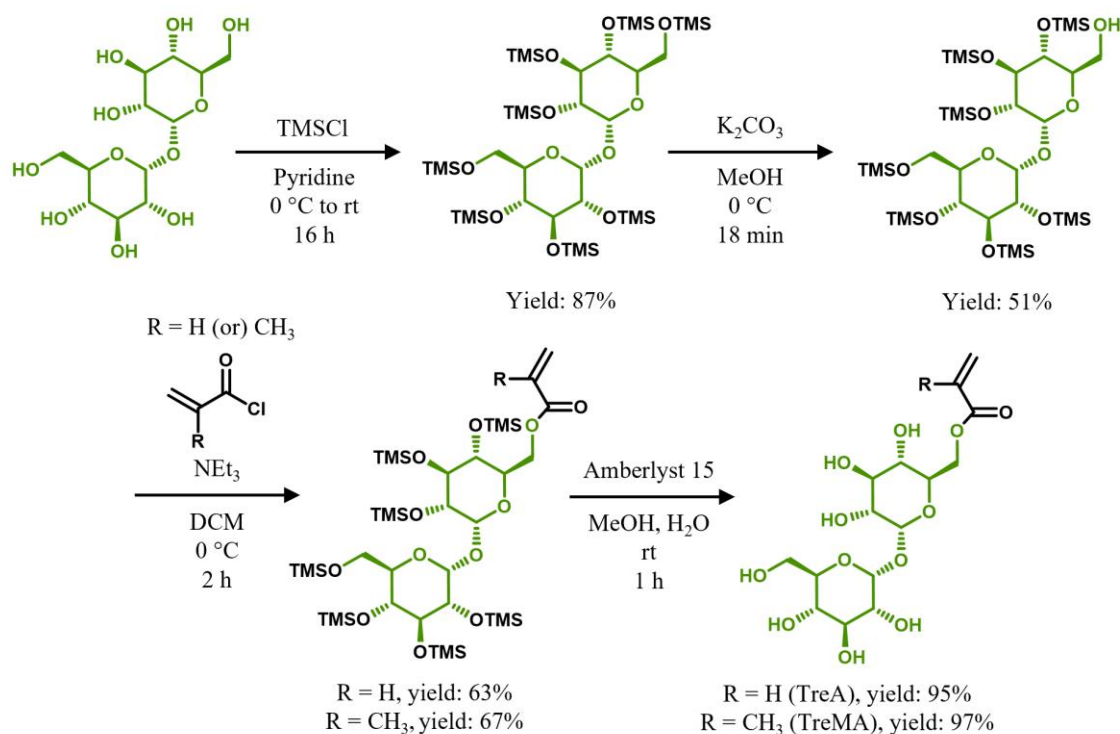


Figure 6. Synthesis of trehalose monomers: 6-*O*-acryloyl-trehalose (TreA) and 6-*O*-methacryloyl-trehalose (TreMA).

The synthesis started with the conversion of anhydrous trehalose to 2,3,4,6, 2',3',4',6'-octa-*O*-trimethylsilyl-trehalose, which afterward underwent regioselective deprotection in methanolic solution at mild basic conditions with a catalytic amount of K₂CO₃. Under such conditions, trimethylsilyl group can be removed from one primary hydroxyl group at C-6 and

2,3,4,2',3',4',6'-hepta-*O*-trimethylsilyl-trehalose can be obtained as a main product by careful control of temperature and reaction time. It can subsequently be isolated using silica gel flash chromatography with 51% of yield. Following a regioselective monoesterification by acryloyl or methacryloyl chloride, hepta-TMS-protected trehalose was transformed into TMS-protected trehalose monomer with (meth)acrylate functionalization at O-6. After purification with silica gel flash chromatography, a colorless solution of 6-*O*-acryloyl-2,3,4,2',3',4',6'-hepta-*O*-trimethylsilyl- α,α' -D-trehalose or 6-*O*-methacryloyl-2,3,4,2',3',4',6'-hepta-*O*-trimethylsilyl- α,α' -D-trehalose was obtained with 63 or 67% of yield, respectively. Finally, Amberlyst 15, an acidic resin, facilitated the final deprotection of the monomer from the remaining TMS groups and allowed for isolation of TreA or TreMA monomer with almost quantitative yield. The overall yields of TreA and TreMA starting from free trehalose until final products were 27 and 29%, respectively.

3.2.2. Synthesis and physicochemical characterization of nanogels

To synthesize trehalose-containing nanogels, the elaborated synthesis procedure described in the previous chapter 3.1 was used. The set of monomers for synthesis of nanogels included four type of monomers: (A) trehalose-incorporating monomer: TreA or TreMA, (B) non-ionic monomer: acrylamide (AM) - primary amide or DMAM – tertiary amide, (C) ionic monomer: 3-acrylamidopropyltrimethylammonium chloride (AMPTMAC) – secondary acrylamide with quaternary ammonium moiety or ATC – acrylate with quaternary ammonium moiety or 4-acrylamidobutanoic acid (4-AMBA) - secondary acrylamide with carboxylic acid group, and (D) crosslinker: MBA – bis-(secondary acrylamide) or poly(ethylene glycol)₄₀₀ diacrylate (PEG₄₀₀DA) – bis-acrylate (**Figure 7A–D**).

The selection of monomers is crucial for the characteristic of nanogels in terms of releasable or non-releasable trehalose as well as network charge. Combining trehalose (meth)acrylate with secondary and primary acrylamides (AM and AMPTMAC or AMBA and MBA) should enable trehalose release at pH 7.4. In turn replacing these acrylamides with tertiary acrylamide (DMAM) and acrylates (ATC and PEG₄₀₀DA), which do not accelerate ester hydrolysis, should not induce trehalose release at pH 7.4. Ionic monomers functionalize nanogels with positive (AMPTMAC or ATC) or negative (AMBA) network charge, and one of the reasons for their introduction was to provide colloidal stability of nanogels. Network charge also offers further possibility of electrostatic binding with bioactive compounds, what could extend nanogels functionality.

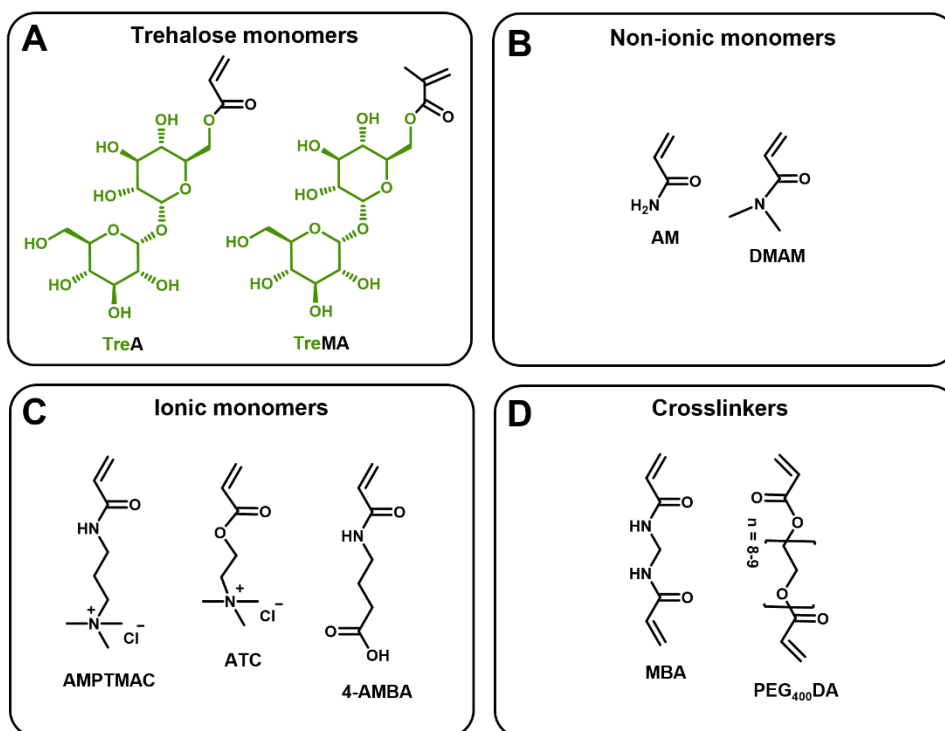


Figure 7. Monomers used for the synthesis of trehalose-containing nanogels. (A) Trehalose monomers: TreA and TreMA. (B) Non-ionic monomers: AM and DMAM. (C) Ionic monomers: AMPTMAC, ATC, and 4-AMBA. (D) Crosslinkers: MBA and PEG₄₀₀DA.

Nanogels TNG1–9 (described in [P4] [59]) were synthesized by varying TreA, AMPTMAC, and AM content to study the effect of nanogels composition on trehalose release profile, cytotoxicity, colloidal stability, and to select the optimal composition of trehalose-releasing cationic nanogels.

The best nanogel formulation according to the study was found in TNG7-AM, which was subjected to further modifications to investigate other related effects. In TNG10-AM, which was just described as TNG in [P5] [60], the cationic AMPTMAC was replaced by carboxylic acid group-bearing 4-AMBA with the aim to synthesize corresponding nanogel with opposite network charge. In TNG7a-AM, TreA was replaced by its methacrylate analogue TreMA to study if trehalose release is influenced by the structure of the acyl moiety, through which trehalose is incorporated within nanogel network. In TNG7b and TNG7c, AMPTMAC was replaced by corresponding acrylate type monomer ATC, while AM was replaced by tertiary acrylamide-type monomer DMAM. Moreover, TNG7c was crosslinked by PEG₄₀₀DA, to exclude MBA, which has secondary acrylamide moieties. The replacement of primary and secondary acrylamide-type monomers by acrylates and tertiary acrylamide was done to remove an accelerating effect on ester hydrolysis in acrylate units, and hence obtain nanogels with covalently bound but non-releasable trehalose, which could serve as biological controls for

trehalose-releasing nanogels. The illustration on how these acrylamide-based neighboring groups influenced the release of trehalose in physiological conditions is shown in **Figure 8**.

The monomer compositions of nanogels are presented in **Table 1**. The majority of trehalose-containing nanogels were designed to have a positive network charge (provided by AMPTMAC or ATC). The main reason is that cationic nanogels would be beneficial for treatment of neurodegenerative diseases in two ways, namely facilitation of BBB crossing *via* the AMT route and possibility of complexation with oligonucleotides. Antisense therapy, using synthetic oligonucleotides, holds promise in combating neurodegenerative diseases by targeting RNA to modify protein synthesis or splicing [74]. It has been shown in the earlier study [P3] [58] that cationic nanogels could effectively complex a-miR21 with high MLC. Hence, cationic trehalose-releasing nanogels could potentially be used for development of dual-functional nanomedicine which would act by autophagy stimulating effect of trehalose and therapeutic effect of oligonucleotide.

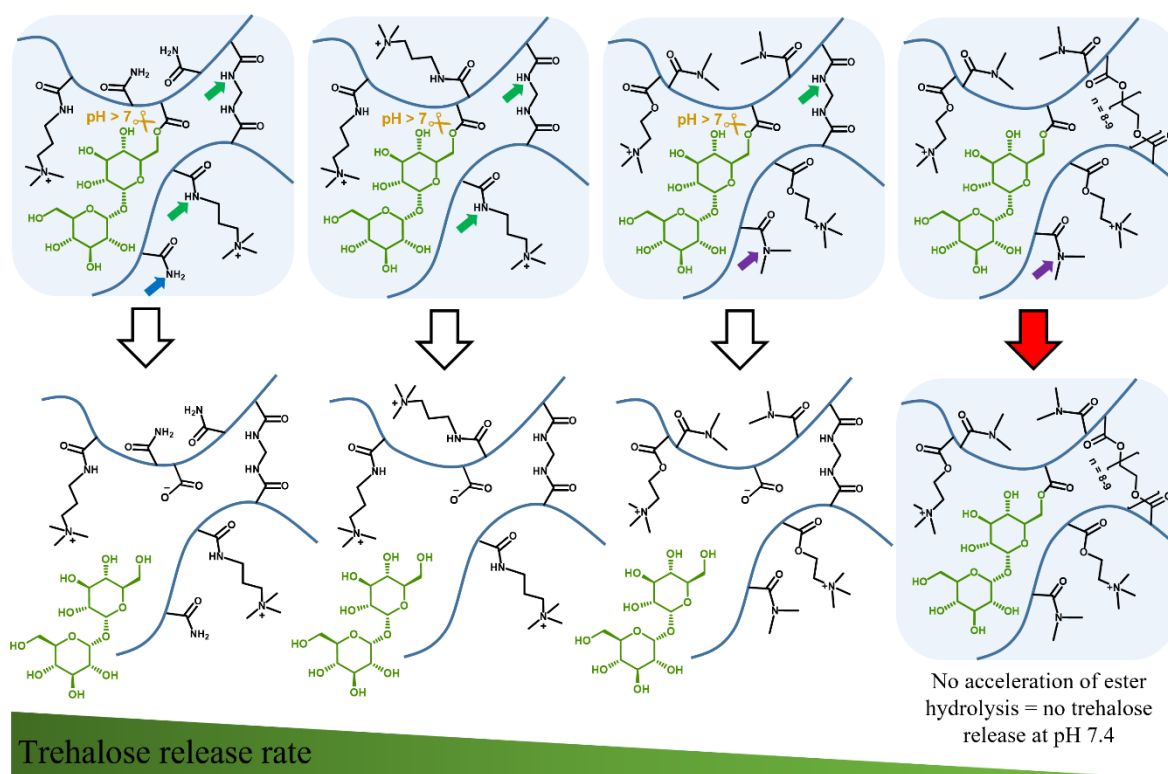


Figure 8. The impact of primary (blue arrow), secondary (green arrow), and tertiary (purple arrow) acrylamide-type co-monomers on ester hydrolysis-mediated trehalose release at pH 7.4.

Table 1. Monomer compositions of trehalose-containing nanogels.

No.	Samples	Trehalose monomers		Non-ionic monomers		Ionic monomers			Crosslinkers		Category*
		TreA	TreMA	AM	DMAM	AMPTMAC	ATC	4-AMBA	MBA	PEG ₄₀₀ DA	
1.	TNG1-AM	++	-	++	-	+++++	-	-	+	-	TR
2.	TNG5-AM	+++++	-	++	-	++	-	-	+	-	TR
3.	TNG6-AM	+++++	-	+++	-	+	-	-	+	-	TR
4.	TNG7-AM	+++++	-	++	-	+	-	-	+	-	TR
5.	TNG2	+++	-	-	-	+++++	-	-	+	-	TR
6.	TNG3	++++	-	-	-	++++	-	-	+	-	TR
7.	TNG4	+++++	-	-	-	+++	-	-	+	-	TR
8.	TNG8	+++++	-	-	-	++	-	-	+	-	TR
9.	TNG9-AM	+++++	-	++	-	-	-	-	+	-	TR
10.	TNG10-AM ^o	+++++	-	++	-	-	-	+	+	-	TR
11.	TNG7a-AM	-	+++++	++	-	+	-	-	+	-	TR
12.	TNG7b	+++++	-	-	++	-	+	-	+	-	TR
13.	TNG7c	+++++	-	-	+	-	+	-	-	++	TNR

Note: TR: trehalose-releasing nanogels, TNR: trehalose-non releasing nanogels. ^oTNG10-AM was denoted as TNG in publication [P5] [60]. Monomer feed: + = < 10% w/w, ++ = 10-20% w/w, +++ = 21-40% w/w, ++++ = 41-50% w/w, and +++++ = >50% w/w.

Table 2. Physicochemical characteristics of trehalose-containing nanogels.

No.	Samples	Yield (%)	CTre (% w/w)	d _H (PdI) in DMEM (nm)	ζ-potential (mV)
1.	TNG1-AM	91	13.9	Aggregated	+35.8
2.	TNG5-AM	77	46.9	213 (0.26)	+32.9
3.	TNG6-AM	70	45.4	187 (0.23)	+37.6
4.	TNG7-AM	73	53.3	115 (0.21)	+22.8
5.	TNG2	85	27.6	162 (0.21)	+38
6.	TNG3	86	33.3	126 (0.18)	+40.9
7.	TNG4	74	46.9	127 (0.18)	+41.5
8.	TNG8	61	57.2	81 (0.19)	+25.5
9.	TNG9-AM	54	58.6	116 (0.22)	-5.7
10.	TNG10-AM	67	57.6	56.6 (0.24)	-17.6
11.	TNG7a-AM	71	35.8	265.6 (0.30)	+24.1
12.	TNG7b	75	53.3	144.9 (0.24)	+30.4
13.	TNG7c	92	51.5	45.0 (0.30)	+22.6

On the other hand, TNG10-AM was synthesized to prolong circulation time of nanogels and accumulate in the plaque by passive targeting due to the inflammation-caused leakiness of endothelial cell lining in the blood vessel walls, particularly in the plaque area [described in P5] [60]. More importantly, the development of anionic trehalose-releasing nanogels can also serve as carriers for cationic compounds or drugs and conjugation with proteins through active esters.

The main goals concerning the physicochemical characteristics of nanogels were to create trehalose-rich nanogels with high content of conjugated trehalose (CTre) of ~50% w/w, while also guaranteeing the sustained release of trehalose and the colloidal stability of nanogels in serum-enriched cell media. The physicochemical characteristics of trehalose-containing nanogels including CTre, d_H with PdI, and ζ -potential can be seen in **Table 2**.

The nanogel yields varied between 54 and 92% and generally higher yields were obtained for nanogels with lower CTre. It can be related to the greater difficulties in polymerization at higher TreA feeding due to the steric hindrance in trehalose monomer caused by its bulky structure. Covalent incorporation of trehalose into nanogels and their purity was confirmed by 1H NMR spectroscopy as shown on the example of TNG10-AM (**Figure 9A**).

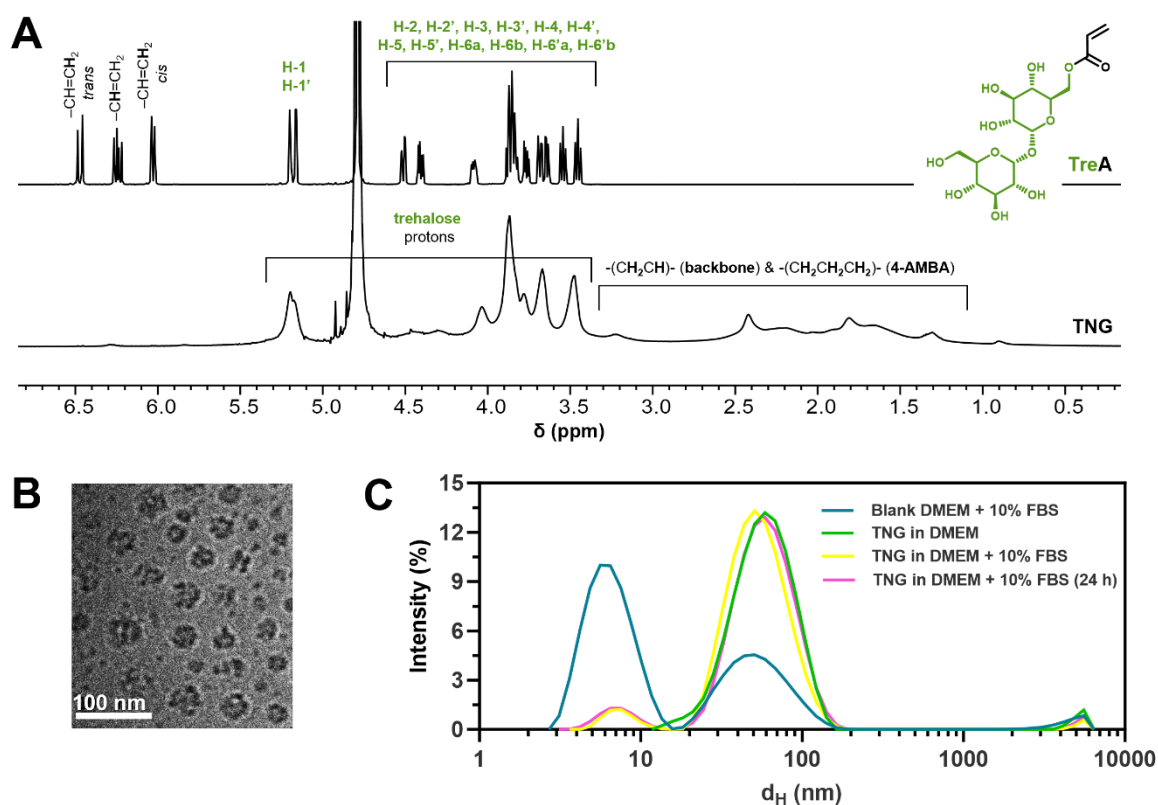


Figure 9. (A) Section of 1H NMR spectra of TreA (top) and TNG10-AM (bottom) proving covalent incorporation of trehalose into TNG10-AM (D_2O , 600 MHz). (B) Cryo-TEM micrograph of TNG10-AM in water. (C) Colloidal stability of TNG10-AM in DMEM + 10% FBS monitored by dynamic light scattering (DLS) measurement. Reproduced with permission from ref. [60]. Copyright 2023 Springer Nature.

The presence of broad signals typical for polymers in the range of 3.3–4.6 and 5.0–5.5 ppm, which are well correlated with proton signals of the trehalose monomer TreA, and the absence of signals from protons of the acrylate group in the range of 6.0–6.5 ppm, both prove successful incorporation of TreA into polymeric network. Additionally, distinct signals from key structural fragments such as methylene groups from 4-AMBA (1.7–1.9, 2.3–2.5 and 3.1–3.3 ppm) and

polymer backbone derived from acrylates and acrylamides (1.1–3.0 ppm) can be easily identified in the spectrum.

The enzymatic assay was utilized to determine the exact content of trehalose (CTre) in nanogels. The principle of enzymatic assay is presented in **Figure 10**. Briefly, trehalose is hydrolyzed to D-glucose by the enzyme trehalase, and then it is phosphorylated by the enzyme hexokinase (HK) and adenosine-5'-triphosphate (ATP) into glucose-6-phosphate (G-6-P) with the simultaneous formation of adenosine-5'-diphosphate (ADP). Nicotinamide-adenine dinucleotide phosphate (NADP^+) then oxidizes glucose-6-phosphate (G-6-P) to gluconate-6-phosphate in the presence of the enzyme glucose-6-phosphate dehydrogenase (G6P-DH), producing reduced nicotinamide-adenine dinucleotide phosphate (NADPH). The amount of D-glucose and, thus, twice the amount of trehalose, are stoichiometric with the amount of NADPH generated in this reaction. In this assay, the amount of NADPH is measured by the increase in its absorbance at 340 nm, for calculating the exact content of trehalose using a generated standard curve of trehalose.

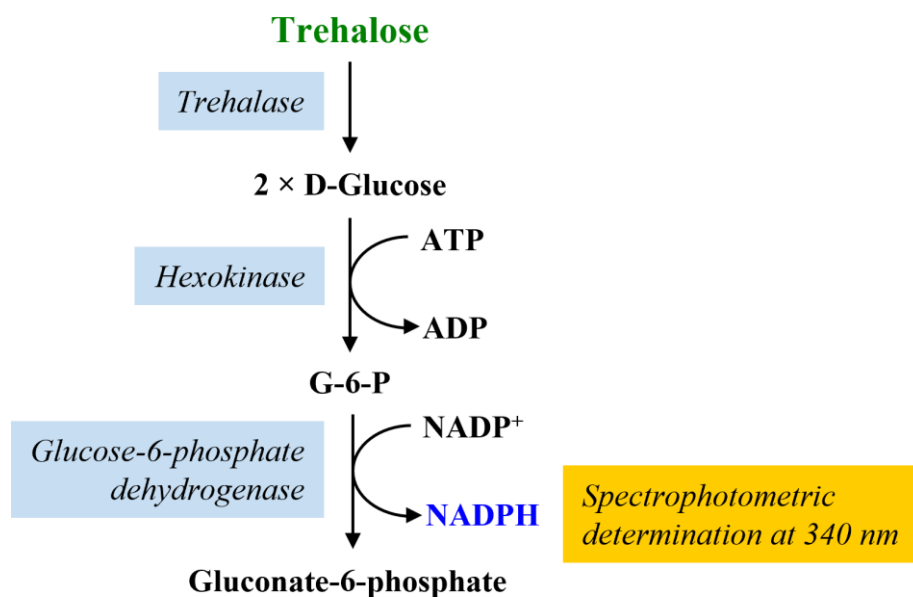


Figure 10. The principle of enzymatic determination of trehalose content using a commercially available enzymatic kit.

TNG2-AM and TNG9-AM showed the lowest and the highest CTre (27.6 and 58.6% w/w, respectively). Generally, the amount of incorporated trehalose correlated well with trehalose monomer feeding. TNG7a-AM, TNG7b and TNG7c were synthesized as counterparts of TNG7-AM. The low content of trehalose in TNG7a-AM but not in TNG7b and TNG7c might be due to the lower relative reactivity of TreMA monomer, in comparison to TreA monomer, and thus causing enrichment of nanogel in other monomers in comparison to the feeding.

The size of trehalose nanogels was determined *via* DLS in DMEM (chosen as a commonly utilized biological medium) and was expressed as the Z-average value. TNG10-AM and TNG7c had the smallest d_H (~50 nm), while the others varied from 80 to 265 nm (PDI range: 0.18–0.3). In general, size of trehalose-releasing nanogels that have been fabricated were in the desired range for long-circulating nanocarriers, which is about 70–200 nm [75]. Cryo-TEM observation revealed that trehalose-releasing nanogels had spherical shape, with average diameter of about 50 nm, which is smaller than the d_H determined by DLS (**Figure 9B**). Nanogels demonstrated varied ζ -potential reaching -5.7 mV for nanogel TNG9-AM containing no ionic monomeric units, -17.6 mV for nanogel TNG10-AM with anionic carboxylic acid moieties and ranging from +22.6 to +41.5 mV for cationic nanogels containing quaternary ammonium cations in the AMPTMAC units. Some negative charge in nanogel TNG9-AM results from the presence of carboxylate anions from the residual photoinitiator moieties. It is important to note that only a nanogel exhibiting a moderate positive or negative are more desired for *in vivo* studies, because a strong positive charge may be toxic to cells, whereas a high negative charge may reduce cell uptake [76], [77].

The colloidal stability of trehalose-containing nanogels were assessed in different media such as water, PBS (pH 7.4), 5% dextrose in normal saline (D5NS), DMEM + 10% FBS, RPMI + 10% FBS, and primary cell medium (low serum) over 72 h [**P4**, *Figure 4 on page 6*] [59]. Nanogels that were colloiddally stable in non-serum containing media were not necessarily colloiddally stable in serum. Particularly, nanogels with trehalose content more than 45% are generally colloiddally stable in serum-containing media. The colloidal stability of nanogels in serum is paramount important, especially for conducting *in vitro* and *in vivo* studies. It must be ensured that nanogels do not aggregate, since this might lead to toxicity to the cells and impair their capacity to perform as nanocarriers. According to literature, cationic nanoparticles could be more cytotoxic than anionic or zwitterionic nanoparticles, which might be due to the affinity of cationic particles to the negatively charged cell membrane [76], [77].

As checked by DLS, the selected nanogels could keep their colloidal stability for at least 24 h of incubation at 37 °C (**Figure 9C** and **P4**, *Figure 5 on page 7*) [59]. Interestingly, trehalose greatly improved the colloidal stability of nanogels, what has been demonstrated by replacing trehalose monomer with 2-hydroxyethyl acrylate (HEA) monomer (hydrophilic monomer with one hydroxyl group). HEA-containing counterpart nanogels were only colloiddally stable in water but they aggregated immediately in PBS (pH 7.4), NS, DMEM, and the most aggregation was found in DMEM + 10% FBS, as described in publication [**P5**] (*Figure S1 in Supplementary Information*) [60]. The additional evidence for beneficial effect of trehalose on colloidal

stability is an example of TNG9-AM, which did not contain additional ionic monomer (the charge came only from the residual initiator), but had high trehalose content, and was colloiddally stable. In contrast, TNG1-AM (with high AM and low TreA) was instantly aggregating. Similarly, TNG2–4 were also colloiddally unstable in biological media due to low content of trehalose [P4, Figure 4 on page 6] [59]. The improved colloiddal stability of nanogels with high content of trehalose might be influenced by its great hydrophilicity and a large number of hydroxyl groups, reflecting a stabilization mechanism based on short-range repulsive hydration forces [78]. Similar beneficial effects of trehalose on the colloiddal stability of polyplexes based on trehalose glycopolymers have been previously hypothesized by Reineke, *et al.* [79], [80]. The colloiddal stability of the cationic trehalose-releasing nanogels in serum has been found to significantly influence the cytotoxicity profile of the nanogels. Colloiddally unstable nanogels were significantly more cytotoxic compared to the stable ones as tested in primary human umbilical vein endothelial cells (HUVECs) up to relatively a high concentration of 1.0 mg/mL [P4, Figure 9 on page 10] [59].

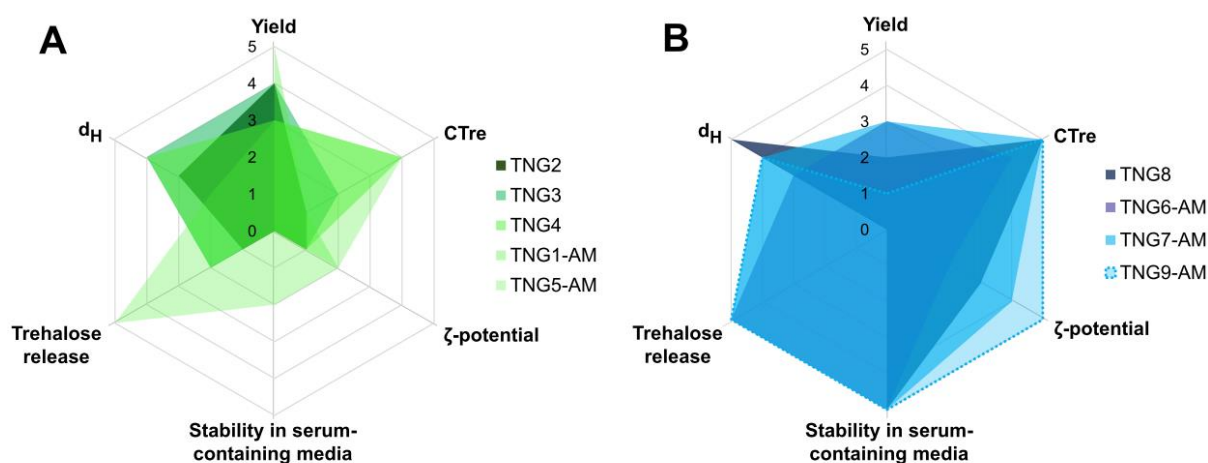


Figure 11. Spider graphs of colloiddally (A) unstable and (B) stable nanogels, showing their characteristics in terms of yield, CTre, ζ-potential, stability in serum-containing DMEM, trehalose release, and d_H. Spider graphs were constructed according to the scoring classifications on a scale from 0 to 5, with 5 being the most desirable. Reproduced with permission from ref. [59]. Copyright 2022 Elsevier.

To compare all physicochemical characteristics of nanogels, a scoring method was employed, in which five parameters including yield, CTre, ζ-potential, stability in serum, d_H, and trehalose release were given a score from 0 to 5, with 5 being the most desirable (P4, Table S3 in *Supplementary Information*) [59]. The spider graphs showed how nanogels differed from each other in terms of their physicochemical characteristics (Figure 11A, B). It is clear that nanogels that contained more than 50% w/w of CTre generally scored the best, with TNG7-AM being the highest score followed by TNG9-AM.

3.2.3. Trehalose release study

Trehalose release was followed by enzymatic determination of trehalose concentration from time-point release experiments, and the resulting release profiles are shown in **Figure 12A-F**. Trehalose release experiments were conducted in 10 mM PBS (pH 6.5, 7.4, and 8.0) at 37 °C, with nanogel concentrations of 0.1 and 1.0 mg/mL. For comprehensive analysis, trehalose release was presented based on concentration and percentage. These two types of analysis allow observation of different aspects of trehalose release. Specifically, release presented as a percentage allows comparison of the release rate, while release presented as a concentration provides information about the nanogel's performance in the context of the amount of released trehalose.

Both, the content and the structure of the acrylamide-type co-monomers significantly affected the hydrolysis rate of ester moieties in acrylate units and thus trehalose release. It is well reflected in trehalose release profile of the following nanogels: TNG2, TNG4, TNG8, TNG5-AM, and TNG7-AM (**Figure 12A, B**). The trehalose release rate from TNG2, TNG4, and TNG8 was considerably decreasing with the increase in TreA and the decrease in acrylamide-type (AMPTMAC) contents. Consequently, even though TNG8 had twice as much conjugated trehalose compared to TNG2 (~57% vs ~28%, respectively), the amount of trehalose released over time was about equal. This suggests that a decrease in the proportion of acrylamide-type monomer units to TreA units resulted in a slower hydrolysis of ester groups in acrylate units, and thus to a slower release of trehalose. Acceleration of ester hydrolysis in acrylate units by acrylamide-type units depends on amide order, and is more prominent for primary amide than for secondary amide, thus the release rate was greatly accelerated when AM was present in nanogel network. It is well observed in release profiles of nanogels TNG4 and TNG5-AM, which contained similar amount of trehalose acrylate, but in TNG5-AM half of AMPTMAC was replaced by AM. For example, after one week, TNG5-AM released approximately 25% more trehalose than TNG4. Unfortunately, although TNG5-AM was the best performing nanogel in terms of trehalose release as it released the highest amount of trehalose per time among all discussed nanogels, it had poor colloidal stability in serum-containing media, where it aggregated immediately. An excellent improvement in colloidal stability was obtained, by increasing TreA content in place of AMPTMAC as was done in nanogel TNG7-AM. Although it slowed down the release rate, higher trehalose content guaranteed that the amount of trehalose released from TNG7-AM was comparable to that released from TNG5-AM.

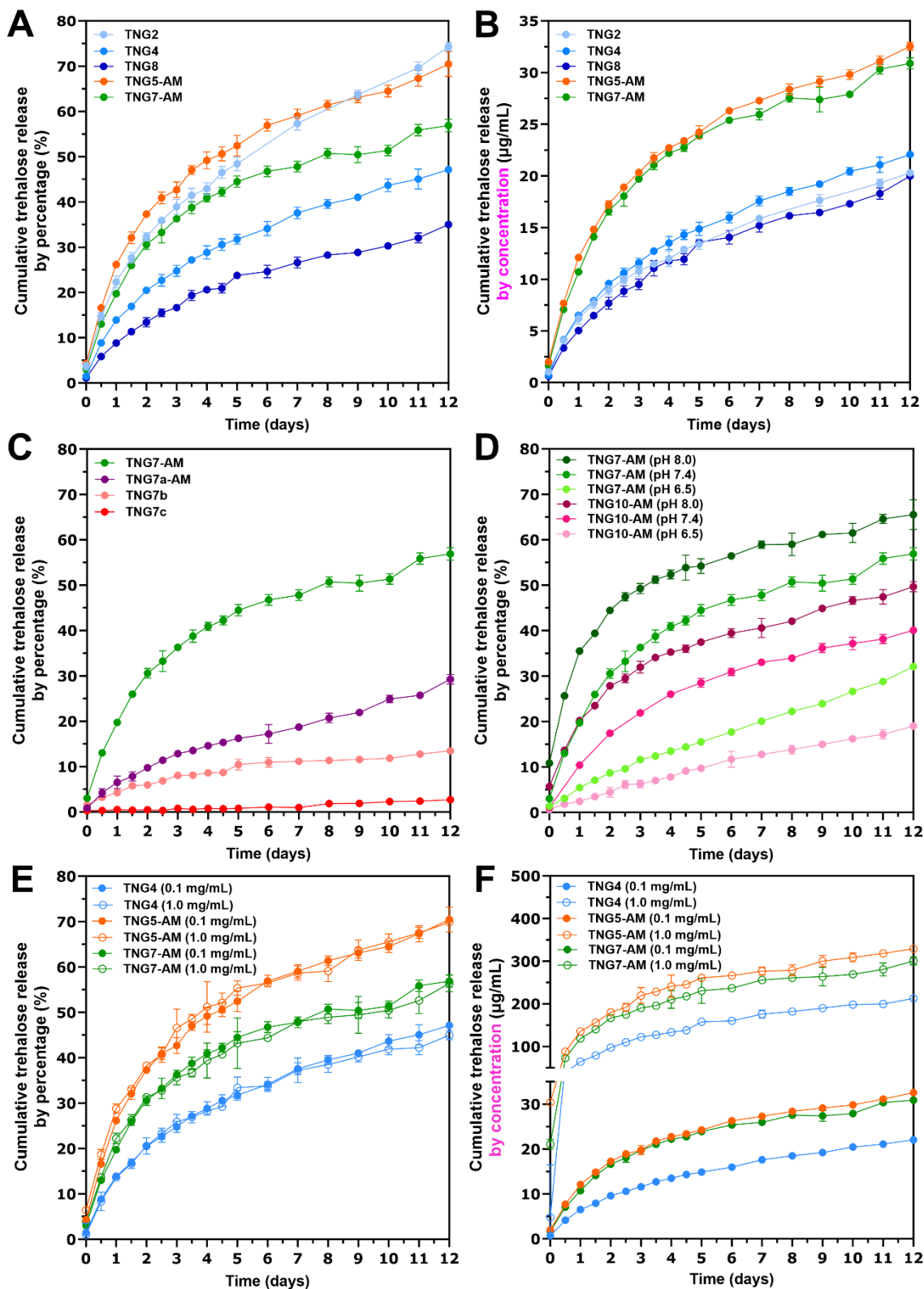


Figure 12. Trehalose release profiles of trehalose-containing nanogels for 12 days in PBS (pH 7.4) at 37 °C. (A, B) Trehalose release profile of TNG2, TNG4, TNG8, TNG5-AM, and TNG7-AM based on (A) percentage and (B) concentration. (C) Trehalose release profile of TNG7-AM and its counterparts (TNG7a-AM, TNG7b, and TNG7c). (D) Trehalose release profile of cationic TNG7-AM and anionic TNG10-AM at different pH (6.5, 7.4, and 8.0). (E, F) Trehalose release profile of TNG4, TNG5-AM, and TNG7-AM at different concentrations (0.1 and 1.0 mg/mL) based on (E) percentage and (F) concentration.

In **Figure 12C** trehalose release profile for TNG7-AM was compared with that of its counterparts TNG7a-AM, TNG7b and TNG7c (**Figure 12C**). First, by looking at TNG7-AM and TNG7a-AM data it can be compared how the structure of the acyl moiety, through which trehalose was incorporated, influence the release of trehalose from nanogels. The percentage of trehalose release was approximately two to three times lower for nanogel TNG7a-AM with trehalose methacrylate units compared to nanogel TNG7-AM with trehalose acrylate units. Specifically, the percentage release from methacrylate *vs.* acrylate containing nanogel reached ~6% *vs.* ~20% after 1 day, ~15% *vs.* ~45% after 6 days and ~25% *vs.* ~55% after 12 days, respectively. The observed differences are consistent with the existing literature indicating that methacrylate-based polymers are by far more resistant to alkaline hydrolysis than acrylate-based polymers [81], [82].

The comparison of release profiles of TNG7-AM, TNG7b and TNG7c (**Figure 12C**), where TNG7b exhibited marginal trehalose release, and TNG7c almost no release of trehalose, shows that modification of the composition of nanogels and replacement of AM and AMPTMAC by co-monomers which do not accelerate ester hydrolysis in acrylate units (tertiary acrylamide DMAM and acrylate type monomer ATC, respectively) leads to the reduction of trehalose release. To completely avoid trehalose release it is important to replace also MBA crosslinker, as the presence of secondary acrylamide moieties in MBA crosslinker in TNG7b was still enough to provide some trehalose release. The almost zero percent of trehalose release was achieved when PEG₄₀₀DA was used for crosslinking TNG7c instead of MBA, thus creating trehalose non-releasing nanogel, which could serve as a control in biological environment.

Two oppositely charged nanogels, TNG7-AM with a quaternary ammonium cation and TNG10-AM with a carboxylic acid group, were included to investigate how network charge of nanogels and pH of the environment influence the release of trehalose from nanogels.

Three distinct pH values (6.5, 7.4, and 8.0), which are considered as biologically relevant, were used to compare the release of trehalose. The results of trehalose release profiles from both nanogels provide a clear pH-dependent release rate, where the higher the pH, the faster the release rate (**Figure 12D**). The release from the cationic nanogel TNG7-AM was significantly faster than that from the anionic counterpart TNG10-AM, which might be due to the differences in local pH within nanogel network. Faster rate of ester hydrolysis in hydrogel network containing positively charged moieties compared to the one with negatively charged groups has also been previously observed in literature [83]. Jo *et al.*, has demonstrated that hydrogel degradation proceeding through an ester moiety cleavage can be modulated by neighboring

amino acids with ca. 12-fold faster hydrolysis in case of network containing positively charged arginine units than that with negatively charged aspartic acid units [83].

The last study on trehalose release assessed comparison of trehalose release from TNG4, TNG5-AM, and TNG7-AM at different concentrations and is presented in **Figure 12E–F**. It revealed that the amount of released trehalose was proportional to nanogel concentration but the release rate was not concentration-dependent (0.1 vs 1.0 mg/mL, **Figure 12E–F**). This property is highly desirable for determining the optimal dose for any *in vitro* or *in vivo* studies. The successful and sustained release of trehalose from the nanogels at pH 7.4, 37 °C is also well evidenced in ^1H NMR spectra, as shown on the example of TNG7-AM (**Figure 13B,C**). With increasing incubation time, the intensity of sharp peaks corresponding to protons of free (released) trehalose was increasing, whereas that of the broad peaks originating from protons of trehalose bound to the nanogel network was decreasing.

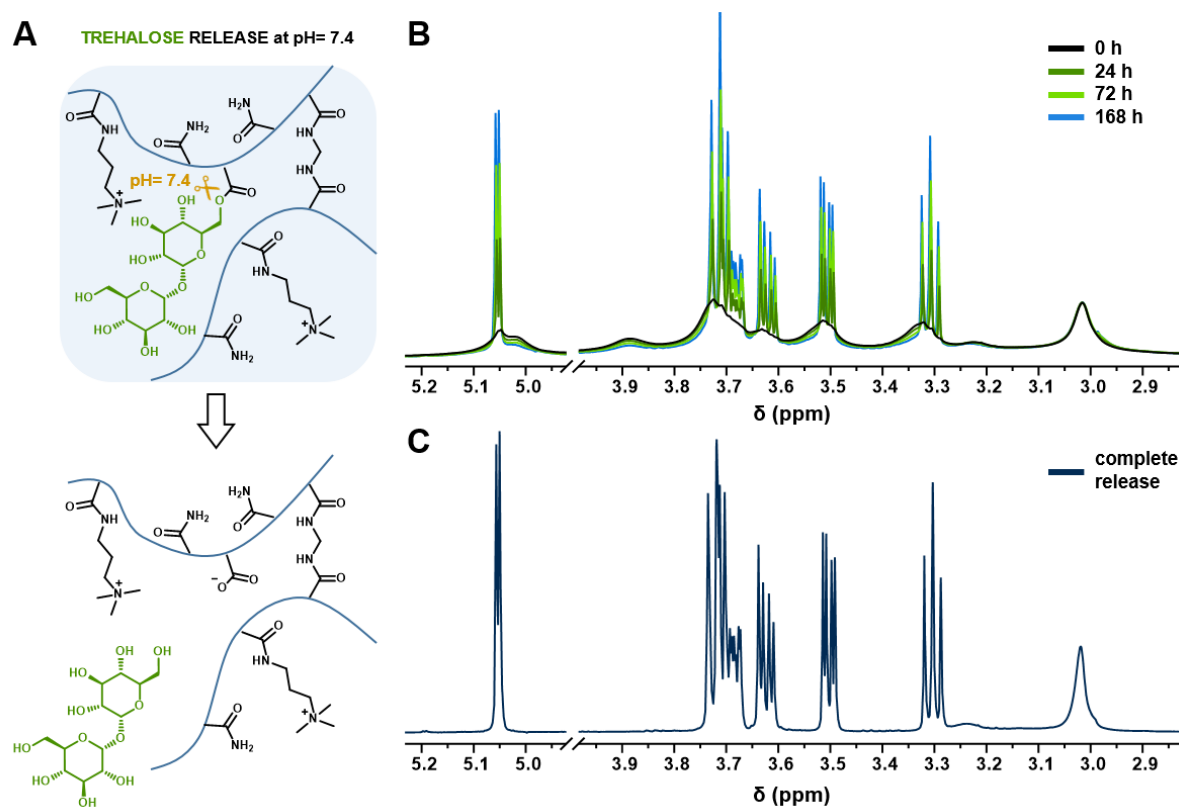


Figure 13. Trehalose release from TNG7-AM (10 mg/mL) evidenced by ^1H NMR spectroscopy. (A) Schematic presentation of trehalose release from the nanogel network *via* the hydrolytic cleavage of the ester bond at pH 7.4. (B) Section of ^1H NMR spectra of TNG7-AM before and during the release of trehalose at pH 7.4, 37 °C. All spectra are normalized to the signal at 3.0 ppm corresponding to $-\text{CH}_3$ protons from AMPTMAC units. (C) Section of ^1H NMR spectrum of TNG7-AM after complete release of trehalose induced by the treatment of TNG7-AM with 1M NaOH at 70°C for 1 h. Reproduced with permission from ref. [59]. Copyright 2022 Elsevier.

The study on trehalose release from TNG7-AM was also extended with an additional experiment involving measurement of ζ -potential upon trehalose release. When ester hydrolysis occurs and the carboxylate ions are formed, the charge switch into the negative ζ -potential should be observed (**Figure 8, 13A**). To prove this hypothesis, the ζ -potential of TNG7-AM in the end of trehalose release experiment as well as after complete release have been measured and the result showed that the ζ -potential of TNG7-AM was significantly reduced from +22.8 mV (before trehalose release) to +4.6 mV (after 12 days at pH 7.4, 37 °C; ~57% of released trehalose) and -15.1 mV (after complete trehalose release) (**Figure 14A, B**).

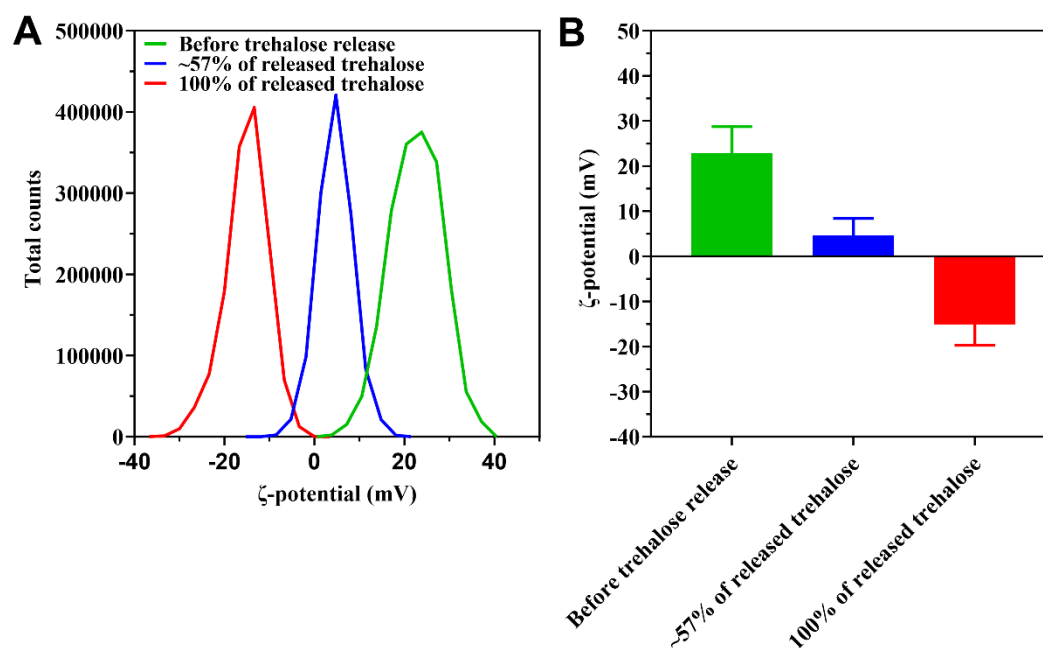


Figure 14. (A, B) ζ -potential measurements of TNG7-AM before trehalose release, after 12 days at pH 7.4, 37 °C (~57% of released trehalose), and after complete trehalose release.

3.3. Biological studies on trehalose-releasing nanogels

Trehalose-releasing nanogels which have been developed and comprehensively studied here represent a significant achievement in the field of trehalose-bearing carriers, because nanocarriers characterized by covalent, yet labile conjugation of trehalose with its proved sustained release at pH 7.4 have not been developed so far. To investigate their further potential, an extensive investigation on their capacity to stimulate autophagy both *in vitro* ([P5] [60]) and *in vivo* ([P4] [59] and [P5] [60]) has been conducted. Initially, the cytotoxic effects of trehalose-releasing nanogels in HUVECs were assessed, followed by hemocompatibility assay in human red blood cells (RBCs). Having established their non-cytotoxic and non-hemolytic property, the study proceeded to examine their ability to stimulate autophagy, both in cell and animal

models. Furthermore, the therapeutic potential of trehalose-releasing nanogels to facilitate lipid efflux-mediated atherosclerosis regression has also been studied.

3.3.1. Autophagy stimulation in *Drosophila* and zebrafish larvae

Two trehalose-releasing nanogels—TNG7-AM and TNG9-AM—were selected for the *in vivo* autophagy stimulation investigation owing to their outstanding characteristics, which was summarized in the spider graphs [P4, Figure 8 on page 10] [59], particularly due to the highest amount of CTre, good colloidal stability in serum, and a reasonable rate of trehalose release. Before conducting autophagy stimulation study, the cellular uptake ability of nanogels in HUVECs was tested to make sure that they could enter into cells by using fluorescein-labelled nanogels. Incubation of nanogels with HUVECs for 3 h at 37 °C, confirmed that both nanogels could be taken up by the cells as observed under CLSM (Figure 15A, B).

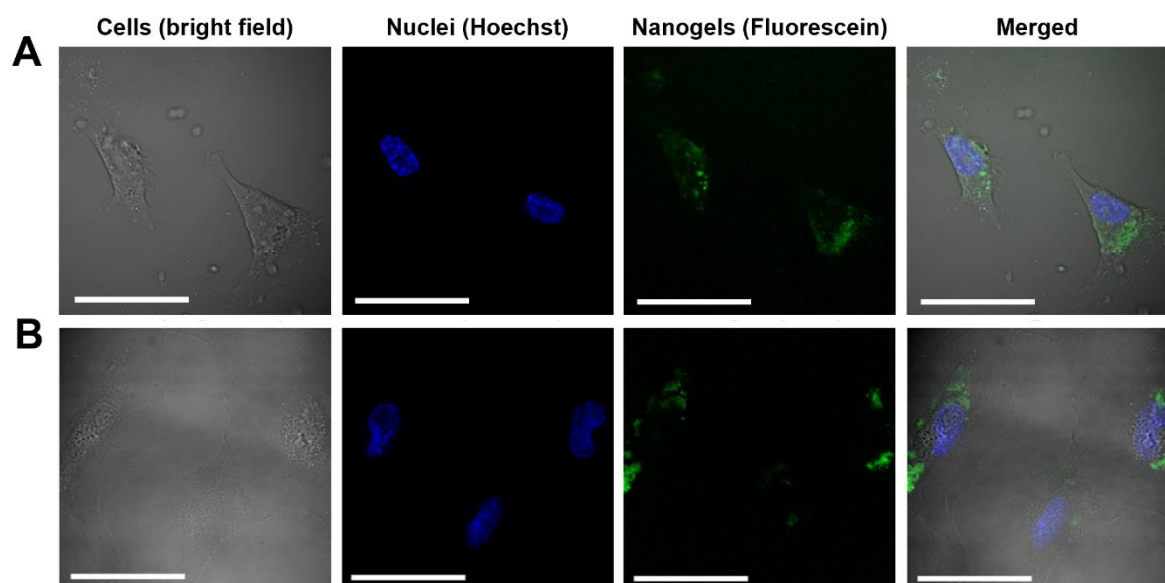


Figure 15. (A, B) *In vitro* cell uptake of (A) TNG7-AM and (B) TNG9-AM by HUVECs observed under confocal laser scanning microscopy (CLSM) (500 µg/mL, 3 h). Brightfield indicates HUVECs, blue color indicates cell nuclei, and green color indicates nanogels (scale bars = 50 µm). Reproduced with permission from ref. [59]. Copyright 2022 Elsevier.

In order to assess the effects of the selected trehalose-releasing nanogels on autophagy stimulation *in vivo*, a well-established zebrafish transgenic reporter line was used to observe the impact of prolonged exposure of those nanogels on the mortality of transgenic zebrafish larvae and their ability to induce autophagy. These studies were conducted by Dr. Máté Varga's group from the Eötvös Loránd University (ELTE), Hungary. The results showed that no significant differences in the mortality of transgenic zebrafish larvae were observed during 4-day treatment (between 1 and 5 days post fertilization – dpf) with 500 µg/mL of TNG7-AM or TNG9-AM.

On the contrary, when exposed to TNG7-AM, the treated larvae demonstrated a considerable increase in autophagic activity as evidenced from the green fluorescent protein (GFP)-microtubule-associated protein 1A/1B-light chain 3 (LC3) signal, but no significant increase in GFP-LC3 signal was observed for TNG9-AM treatment (**Figure 16A, B**). Furthermore, an elevated degree of Sqstm1/p62 degradation was spotted in larvae treated with TNG7-AM, reflecting an increase in autophagic activity.

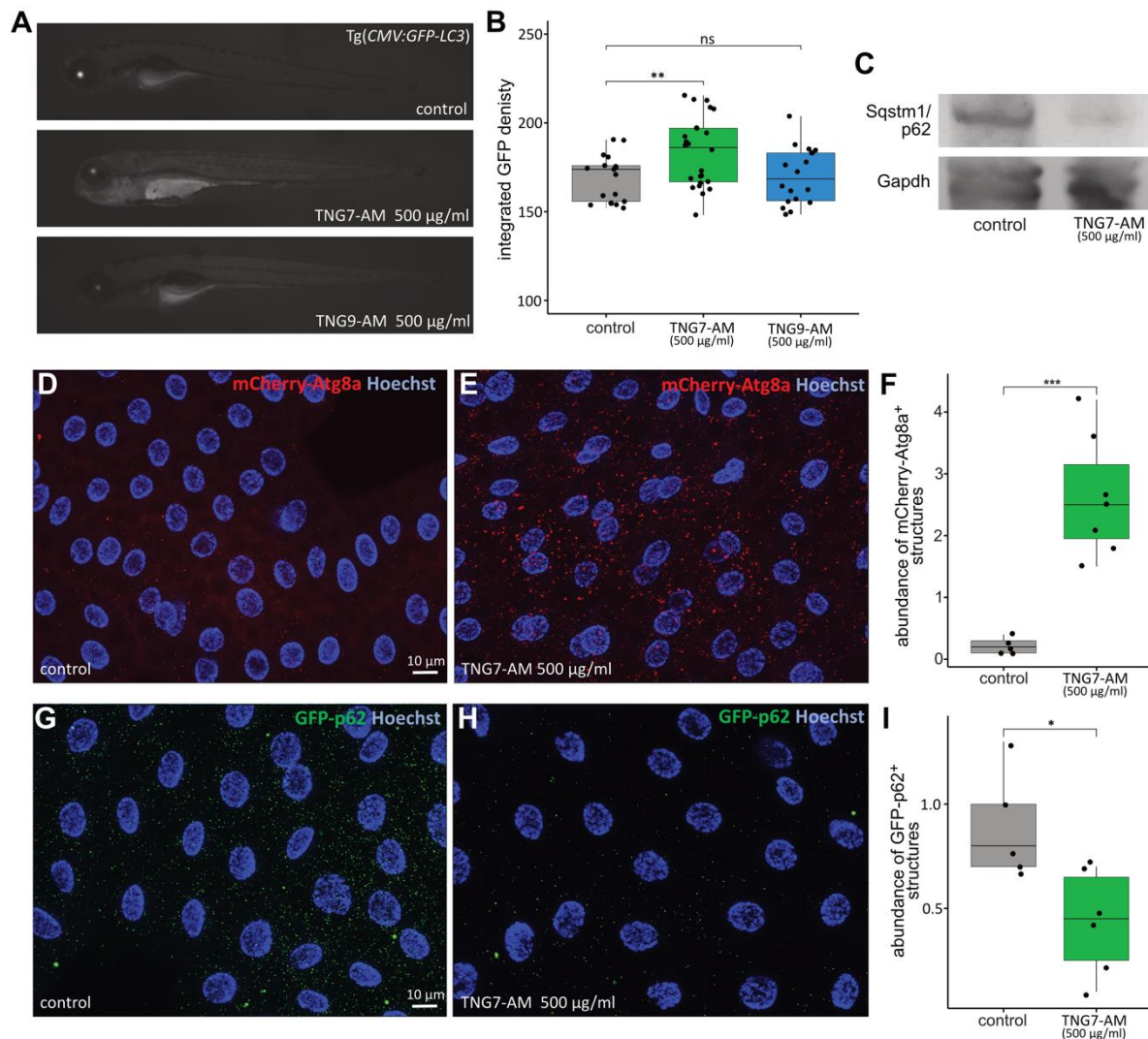


Figure 16. *In vivo* autophagy-enhancing effects of trehalose-releasing nanogels. (A-B) Transgenic zebrafish larvae of the autophagy-reporter line Tg(*CMV:GFP-Lc3*) showed significantly enhanced fluorescence after 4 days of treatment with TNG7-AM, but not with TNG9-AM. (C) Zebrafish treated with TNG7-AM also showed a decrease in Sqstm1/p62 accumulation. (D-F) In the fat bodies of *3xmCherry-Atg8a* transgenic *Drosophila* larvae raised on TNG7-AM-containing medium, the number of mCherry-Atg8a-positive structures increases. (G-I) Fat bodies of *GFP-p62* transgenic animals show a marked decrease in the number of GFP-p62-positive structures, as compared with control. Reproduced with permission from ref. [59]. Copyright 2022 Elsevier.

To further assess the potential of TNG7-AM in enhancing autophagy *in vivo*, *Drosophila* larvae were cultivated on a medium supplemented with the nanogel. Following continuous exposure for 3 days, significantly increased levels of mCherry-Atg8a-positive structures were observed

in the fat bodies of transgenic *3xmCherry-Atg8a* larvae (**Figure 16D–F**). The *Atg8a* protein is one of the most effective markers used to trace autophagy in different organisms, including *Drosophila* [84]. A similar treatment regimen also led to a reduction in the abundance of GFP-p62-positive structures in the fat bodies of *GFP-p62* larvae (**Figure 16G–I**). These findings imply that prolonged exposure to TNG7-AM can enhance autophagic activity in *in vivo* systems without any observable toxicity.

3.3.2. Autophagy stimulation for atherosclerosis treatment in mice

Atherosclerosis is one of the diseases linked to autophagy dysfunction. This chronic disease is associated with plaque development and narrowing of blood vessels due to inflammation in the arterial walls caused by lipid deposition. The EPR effect facilitates nanocarriers to cross the disrupted endothelial lining/barrier at the site of atherosclerosis. In addition, many literature reports showed that negatively charged nanocarriers have an extended circulation time compared to positively charged nanocarriers [85], [86], [87]. Therefore, TNG10-AM or just called as “TNG” in [P5] [60] was synthesized following the formulation of TNG7-AM but replacing the cationic monomer AMPTMAC with anionic monomer 4-AMBA (**Figure 17A**). The effectiveness of this nanogel to stimulate autophagy was evaluated in *in vitro* and *in vivo* studies, and were conducted by Prof. Wei Wu’s group from Chongqing University, China.

Before investigating autophagy-inducing potential of TNG10-AM *in vivo*, it is also crucial to first examine its effects *in vitro*. The *in vitro* study was conducted in macrophage-derived foam cells. These macrophages are a particular type of macrophages in blood vessel walls that ingest low-density lipoproteins and accumulate lipids in their cytosol, giving them a foamy appearance. The results from Western blot and fluorescence microscopy showed that TNG10-AM, at a concentration equal to 100 μ M of trehalose, was more effective than 100 μ M of free trehalose in recovering autophagy in foam cells. This was demonstrated by an increase in the LC3-II/LC3-I ratio and a decrease in the p62/GAPDH level when compared to the control foam cells. In addition to its autophagy-inducing potential, TNG10-AM treatment could decrease lipid deposition and reactive oxygen species (ROS) generation in foam cells. This effect was likely attributed to the autophagic activity and antioxidant property of trehalose.

Finally, to assess TNG10-AM efficacy for inducing autophagy and reducing plaque progression *in vivo*, TNG10-AM and free trehalose were administered intravenously (at doses of 16 mg/kg and 2.5 g/kg, respectively) every three days to ApoE^{-/-} mice with additional high-fat diet (HFD) for 30 days (**Figure 17B**).

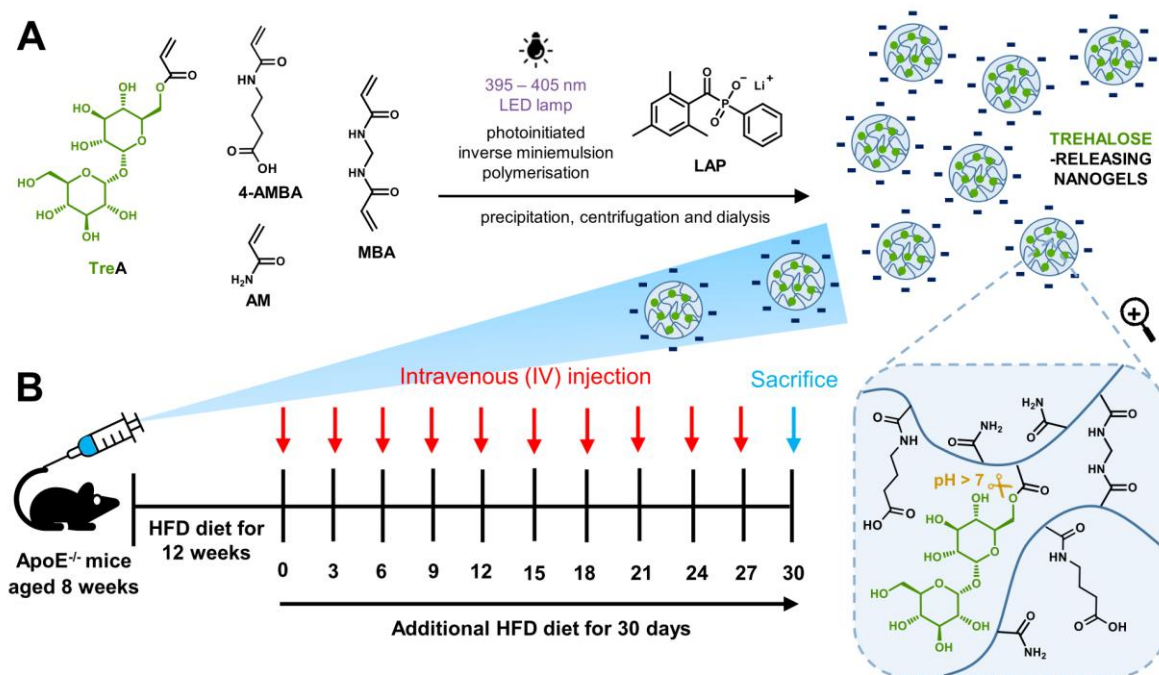


Figure 17. (A) The synthesis of anionic trehalose-releasing nanogels (TNG10-AM), and (B) timeline for ApoE^{-/-} mice pretreatment and systemic administration of TNG10-AM *via* the tail vein. Reproduced with permission from ref. [60]. Copyright 2023 Springer Nature.

After one month of treatment, TNG10-AM demonstrated a significant anti-atherosclerosis effect, reducing the overall plaque area by approximately 60%, surpassing the efficacy of free trehalose. On the other hand, analysis of p62 and LC3 expressions in atherosclerotic plaque areas indicated that TNG10-AM induced a substantial decrease in p62 level (over 50% reduction) and a nearly four-fold increase in LC3 level, indicating its significant autophagy induction. Free trehalose also promoted autophagy in atherosclerosis but to a lesser extent than TNG10-AM. In addition, TNG10-AM treatment effectively reduced macrophage count in the plaques, suggesting its potential to enhance plaque stability and impede atherosclerosis progression more efficiently than free trehalose. The fact that TNG10-AM was used at a dosage which was around 1500× lower than that of free trehalose demonstrated the potential use of nanocarriers to increase bioavailability, cell internalization, and efficacy of free trehalose to treat impaired autophagy-related diseases, such as atherosclerosis. This study is the first report on using nanogels as trehalose carriers to treat atherosclerosis.

The results also showed that Cy5-labelled TNG10-AM displayed a notable accumulation in atherosclerotic plaques, which exceeded the accumulation of free Cy5. However, both were primarily accumulated in the liver compared to other organs, highlighting the liver's role as the major metabolic organ (**Figure 18A–D**). Furthermore, the pharmacokinetics study confirmed that after 24 h, free Cy5 was almost entirely removed from the blood, while Cy5-labelled

TNG10-AM remained about 30% of the initial, which displayed a long-circulating property. TNG10-AM had a half-life ($t_{1/2}$) of around 9 h (**Figure 18E**).

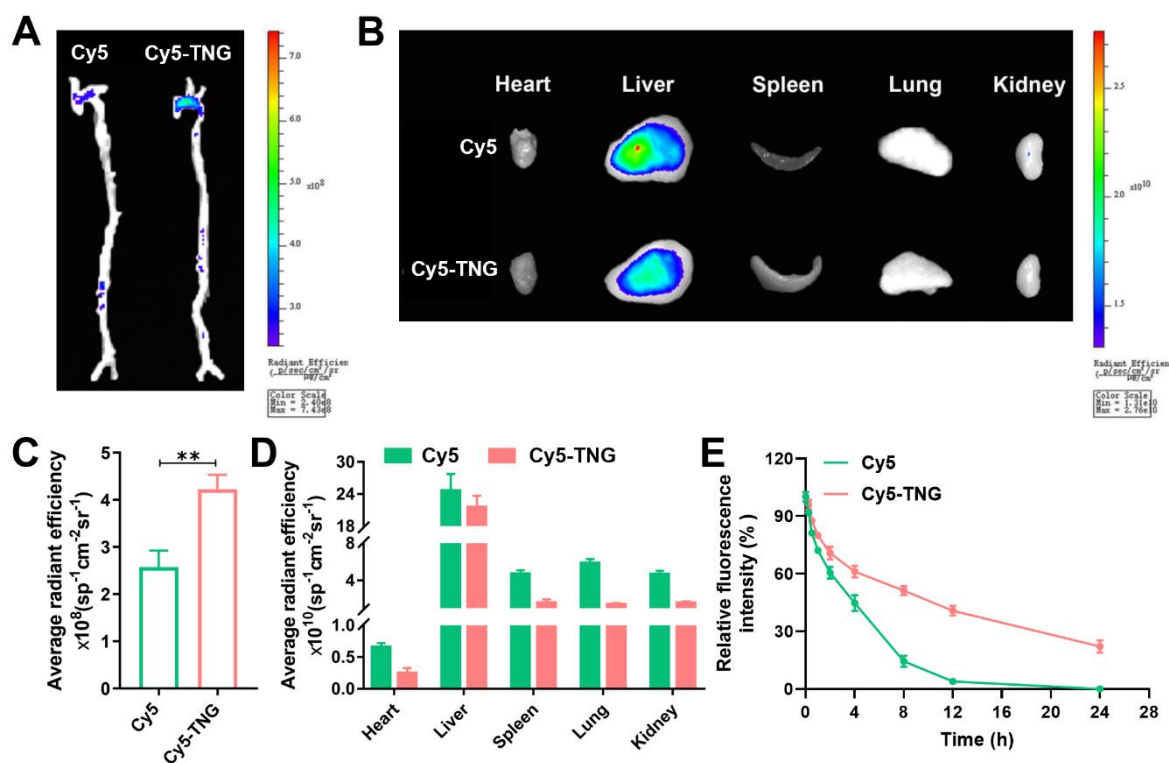


Figure 18. (A) The *ex vivo* fluorescence images of the aorta and (B) quantitative analysis of fluorescence signals accumulated in the aorta of ApoE^{-/-} mice after 24 h of intravenous (IV) administration with Cy5-TNG and free Cy5. (C, D) The *ex vivo* biodistribution images of Cy5-TNG and free Cy5 in major organs (heart, liver, spleen, lung, and kidney). Data are presented as mean \pm SD, $n = 3$, ns: no significance, $*p < 0.05$ and $**p < 0.01$. (E) *In vivo* pharmacokinetics evaluation of nanogels in mice. Adapted with permission from ref. [60]. Copyright 2023 Springer Nature.

3.4. Fluorescent labeling of nanogels for imaging in biological studies

Various imaging functionalities can be employed to utilize nanocarriers as diagnostic agents, and fluorescent labeling is among the most common ones, particularly due to their versatility, sensitivity and quantitative capabilities. The incorporation of fluorescent agents to nanocarriers can be done either by physical loading or chemical conjugation [88]. Herein, to enable fluorescent imaging in biological studies fluorescent dyes were incorporated to nanogels by the chemical conjugation using two different approaches (**Figure 19A, B**).

In the first approach, commercially available fluorescent monomer (fluorescein *O*-acrylate, **Figure 19A**) was incorporated during polymerization, yielding fluorescein-labelled nanogels in one step. In the second approach, fluorescent labeling was carried out in post-polymerization route using reactive moieties installed in nanogels. Specifically self-made 4-AMBA-sulfo-NHS monomer (**Figure 19B**) was employed during polymerization to create sulfo-NHS-activated

nanogels. These nanogels were then reacted with sulfo-Cy5-amine to form an amide bond and yield Cy5-labelled nanogels.

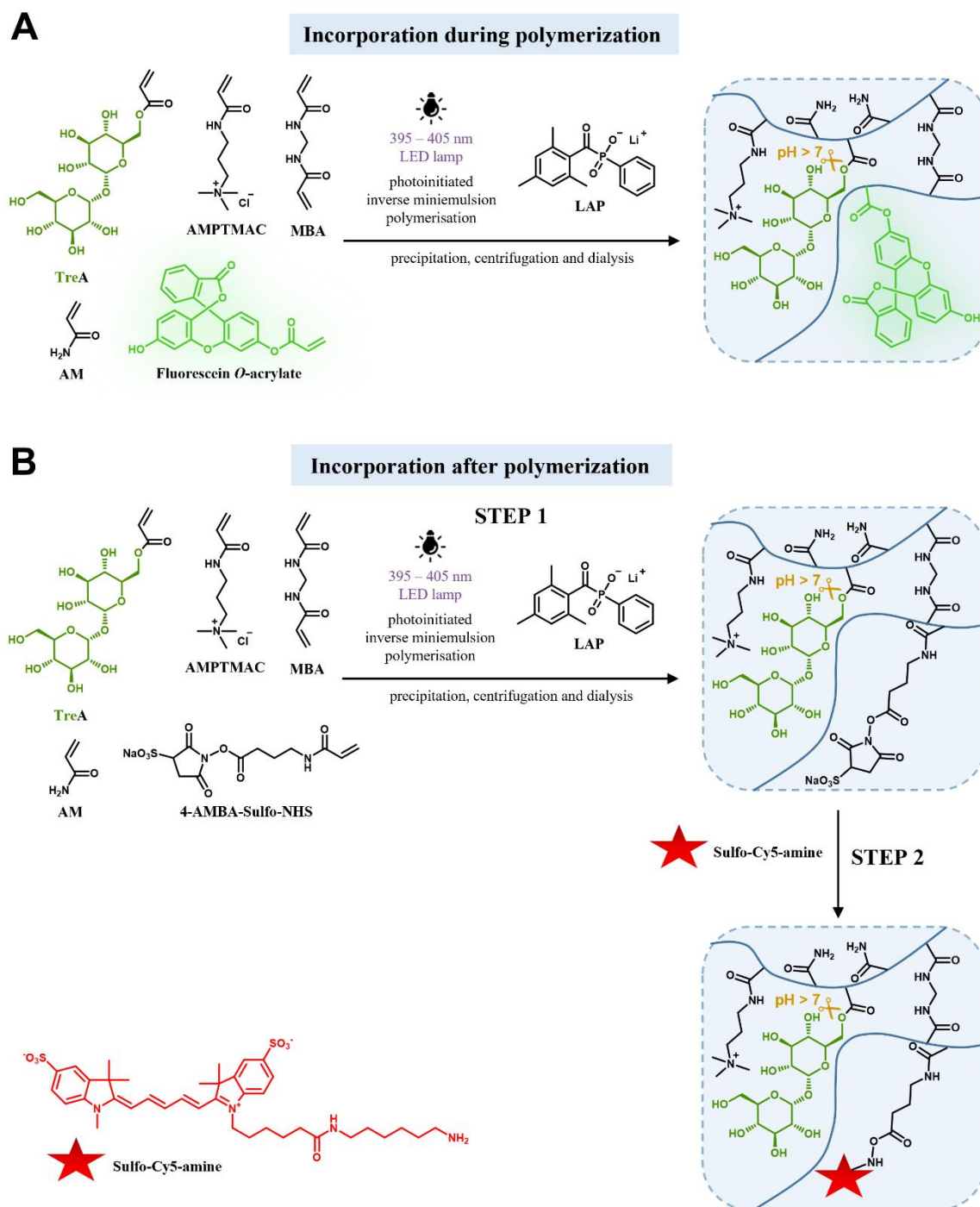


Figure 19. (A, B) The synthesis of fluorescently-labelled trehalose-releasing nanogels using (A) fluorescein *O*-acrylate and (B) sulfo-Cy5-amine as green and red fluorescent agents, respectively.

In the beginning of the study, fluorescein *O*-acrylate was used for fluorescent labeling of nanogels, but two main drawbacks were found using this fluorescent probe. First of all, this fluorescent monomer is not well soluble in water. Therefore, in order to make it soluble in the

aqueous phase, it was required to add DMSO (10% v/v), yet it could only dissolved to a maximum of 0.5% w/w. Secondly, fluorescence of fluorescein is pH dependent and depends on its protonation state, which is defined by its three pK_a values ($pK_{a1} \sim 2.1$, $pK_{a2} \sim 4.3$, and $pK_{a3} \sim 6.5$) (**Figure 20**) [89]. The most deprotonated form, which is dianion, exhibits the highest fluorescence among all fluorescein forms, with fluorescence intensity significantly greater than monoanion form [90]. In fluorescein *O*-acrylate, acrylate functionalization is attached to one of phenolate group, and thus it can be deprotonated only to monoanion. It renders its relatively poor fluorescence. Both those drawbacks - low incorporation due to the solubility issue and rather low fluorescence intensity, forced to use a relatively high concentration of nanogels in biological experiments (500 $\mu\text{g/mL}$, in confocal imaging) in order to be detected (**Figure 15A, B**).

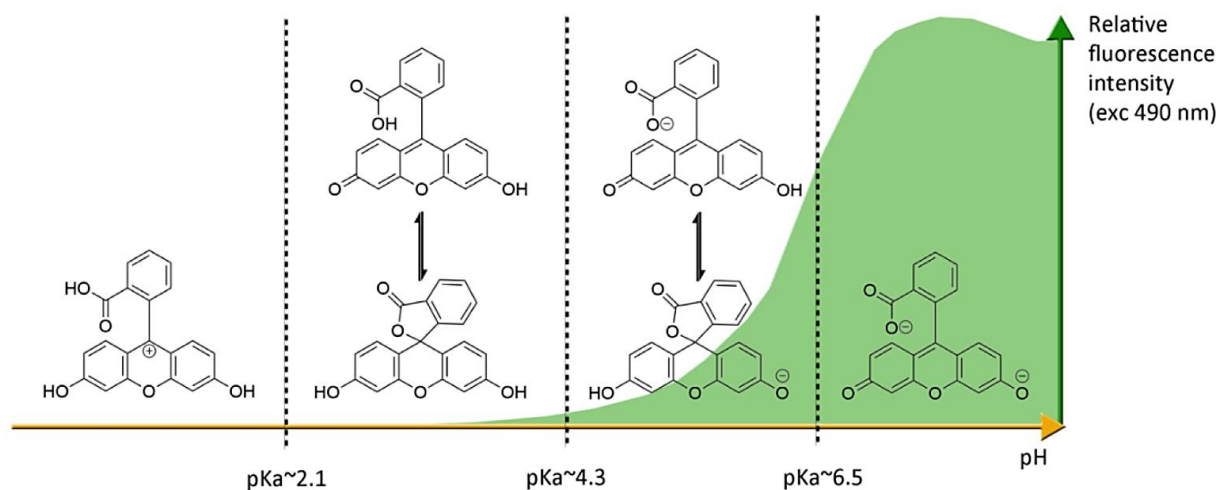


Figure 20. Ionic forms of fluorescein and their relative fluorescence intensities. At neutral pH and under excitation at 490 nm, the most fluorescent dianionic form of fluorescein takes prominence over other forms. Below $\text{pH} = pK_a \sim 6.4$, monoanionic fluorescein displays a blue-shifted absorption followed by drastic decrease of fluorescence. At even lower pH, neutral and further cationic forms of fluorescein become non-fluorescent under irradiation at 490 nm. Reproduced with permission from ref. [89] under the terms of the CC BY 4.0 license. Copyright 2020 The Authors, published by Multidisciplinary Digital Publishing Institute.

In contrast, the second approach was for several reasons much better to create fluorescently-labelled nanogels. First, the fluorescence of Cy5-labelled nanogels were not dependent on pH and. Secondly, nanogels had much higher fluorescent intensity, so it was possible to use a relatively low concentration of nanogels for confocal imaging. Another advantage is conjugation through amide bond, which is more resistant to cleavage through hydrolysis and prevents leaking of the fluorescent dye from nanogels. This strategy is also more versatile as it enables nanogels labeling with various fluorescent moieties. The fluorescence excitation (Ex) and emission (Em) spectra of both fluorescein and Cy5-labelled trehalose-releasing nanogels

can be seen in **Figure 21A, B**. Fluorescein-labelled nanogels showed λ_{Ex} and λ_{Em} maximum at 491 nm and 519 nm, respectively, while Cy5-labelled nanogels showed λ_{Ex} and λ_{Em} maximum at 649 nm and 673 nm, respectively.

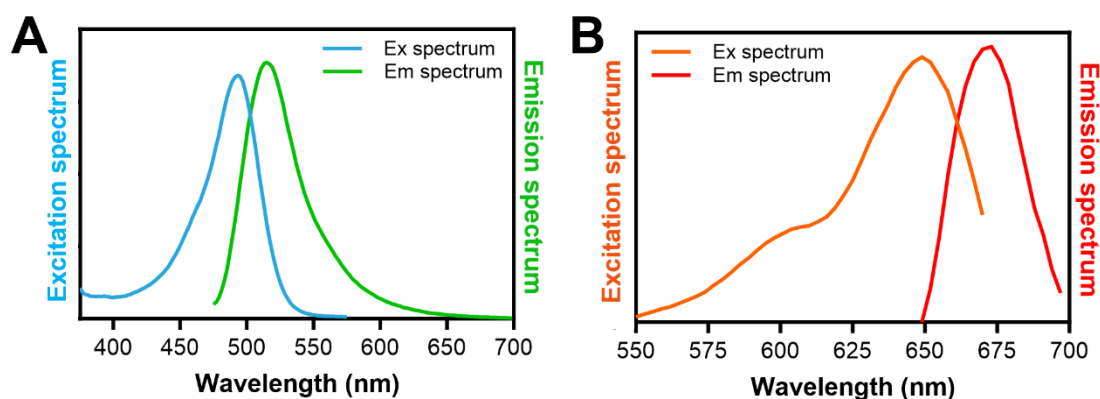


Figure 21. (A, B) Excitation and emission spectra of fluorescently-labelled trehalose-releasing nanogels. (A) Fluorescein-labelled TNG7-AM showed λ_{Ex} and λ_{Em} maximum at 491 nm and 519 nm. (B) Cy5-labelled TNG7-AM showed λ_{Ex} and λ_{Em} maximum at 649 nm and 673 nm.

Sephadex G25 superfine-based gel filtration technique was used to purify the Cy5-labelled cationic and anionic trehalose-releasing nanogels (TNG7-AM and TNG10-AM, respectively) from unconjugated Cy5. Surprisingly, it has been found that both nanogels show different behavior. It can be seen from **Figure 22A, B** that the cationic Cy5-labelled nanogel had a specific interaction with sephadex G25 superfine compared to the anionic counterpart, which might suggest that the conjugation reaction failed in case of the cationic nanogel. In order to confirm the successful Cy5 conjugation in the cationic nanogel TNG7-AM, free sulfo-Cy5-amine in equimass concentration was passed through the sephadex G25 superfine for comparison. It was shown that free sulfo-Cy5-amine left the column with delay and was collected in fractions 7–11 (**Figure 22C**), thus confirming the successful conjugation of Cy5 into TNG7-AM. To further confirm the successful Cy5 conjugation, the cationic Cy5-labelled nanogel was incubated with 10% FBS for one hour before being introduced to the sephadex G25 superfine. Strong interaction of Cy5-labelled nanogel with serum proteins reduced nanogel interaction with the sephadex G25 superfine. Consequently, there was a substantial recovery of Cy5-labelled nanogel, similar to the anionic counterpart, and nanogel was collected in the same fractions (fractions 1–5, figure not shown).

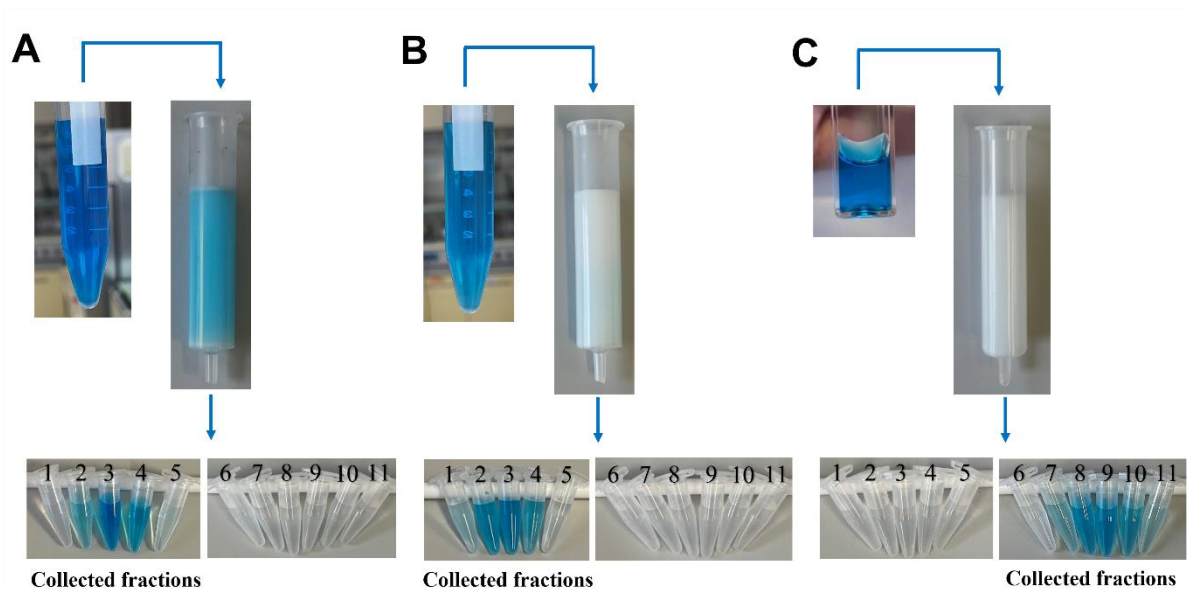


Figure 22. (A) Interaction between cationic Cy5-labelled trehalose-releasing nanogels with sephadex G25 superfine in a desalting column. (B, C) No significant interaction between (B) anionic Cy5-labelled trehalose-releasing nanogels as well as (C) free sulfo-Cy5-amine with sephadex G25 superfine in a desalting column.

Fluorescently-labeled nanogels have been included into three different biological studies. In the first study, it was possible to use fluorescein-labelled nanogels for *in vitro* cell uptake in HCT 116 colon cancer cell line to confirm the successful delivery of miRNA (**Figure 5D**). In the second study, fluorescein-labelled cationic and anionic trehalose-releasing nanogels were used for *in vitro* cell uptake study in primary HUVECs (**Figure 15A, B**). In the last study, Cy5-labelled TNG10-AM was used for *in vivo* plaque targeting, biodistribution, and pharmacokinetics study in atherosclerotic mice models (**Figure 18A–E**).

4. Summary and conclusions

Trehalose is currently used in many biomedical applications, and has a promising potential as autophagy inducer. The construction of covalent, yet hydrolytically-labile at pH 7.4 conjugation of trehalose into nanogels developed as a part of the presented doctoral dissertation is expected to improve its bioavailability and efficacy. The use of FRP in inverse miniemulsion was proved to be suitable method to fabricate uniformly spherical nanogels with appropriate size and plausible yields. Trehalose was covalently conjugated within the polymer network *via* an ester bond, of which the specific location enabled its cleavage under physiologically-relevant conditions resulting in trehalose release. Trehalose release profiles were shown to be dependent on the content and the structure of acrylamide-type units. The lower the percentage of acrylamide-type monomer units in the polymeric network, the slower the release of trehalose from nanogels. The accelerating effect on trehalose release mediated by ester hydrolysis was observed to be more prominent for primary amides than for secondary amides, while it was not observed for tertiary amides. The structure of the acyl moiety, through which trehalose is incorporated within nanogel network, also influenced trehalose release from nanogels. It was found that trehalose release was faster from nanogels containing trehalose acrylate units in comparison to nanogel with trehalose methacrylate units. The network charge of nanogels also influenced trehalose release rate. Cationic nanogels exhibited faster trehalose release than its anionic counterpart, possibly due to the difference in the local pH within the nanogel network. Additionally, trehalose release was depended on pH, with higher pH levels leading to faster release rate. Finally, trehalose release rate does not appear to be concentration-dependent according to the results from three selected nanogels. This property is highly desirable for determining the optimal dose for any *in vitro* or *in vivo* studies. Trehalose presence in nanogels greatly improved their colloidal stability.

As a result of the study, thirteen trehalose-containing nanogels have been successfully synthesized, of which twelve can be classified as trehalose-releasing nanogels and one as trehalose non-releasing nanogel. They were characterized by d_H ranging from 57 to 266 nm and positive or negative zeta potential depending on the charge of the incorporated ionic moieties. The selected trehalose-releasing nanogels had high trehalose content (~50% w/w CTre), were colloidally stable in serum-enriched cell media, non-cytotoxic to HUVECs, and non-hemolytic to human RBCs. More importantly, trehalose-releasing nanogels could significantly induce autophagy in transgenic zebrafish and *Drosophila* larvae and they demonstrated the therapeutic

effects of autophagy stimulation in promoting lipid efflux and plaque reduction in a mouse model of atherosclerosis.

The study was of a high degree of novelty as such trehalose-releasing nanogels had not yet been created and tested its autophagy stimulation effects before. Moreover, it represents a significant achievement in the field of trehalose-bearing carriers, because nanocarriers characterized by covalent, yet labile conjugation of trehalose with its proved sustained release at pH 7.4 have not been developed so far.

5. References

- [1] M. J. Mitchell, M. M. Billingsley, R. M. Haley, M. E. Wechsler, N. A. Peppas, and R. Langer, "Engineering precision nanoparticles for drug delivery," *Nat. Rev. Drug. Discov.* 2021, DOI: 10.1038/s41573-020-0090-8.
- [2] A. P. Singh, A. Biswas, A. Shukla, and P. Maiti, "Targeted therapy in chronic diseases using nanomaterial-based drug delivery vehicles," *Signal. Transduct. Target. Ther.* 2019, DOI: 10.1038/s41392-019-0068-3.
- [3] D. Peer, J. M. Karp, S. Hong, O. C. Farokhzad, R. Margalit, and R. Langer, "Nanocarriers as an emerging platform for cancer therapy," *Nat. Nanotechnol.* 2007, DOI: 10.1038/nnano.2007.387.
- [4] J. H. Lee and Y. Yeo, "Controlled drug release from pharmaceutical nanocarriers," *Chem. Eng. Sci.* 2015, DOI: 10.1016/j.ces.2014.08.046.
- [5] S. Kumar, N. Dilbaghi, R. Saharan, and G. Bhanjana, "Nanotechnology as emerging tool for enhancing solubility of poorly water-soluble drugs," *Bionanoscience* 2012, DOI: 10.1007/s12668-012-0060-7.
- [6] S.D. Li and L. Huang, "Pharmacokinetics and biodistribution of nanoparticles," *Mol. Pharm.* 2008, DOI: 10.1021/mp800049w.
- [7] N. Hoshyar, S. Gray, H. Han, and G. Bao, "The effect of nanoparticle size on in vivo pharmacokinetics and cellular interaction," *Nanomedicine* 2016, DOI: 10.2217/nmm.16.5.
- [8] M. Chamundeeswari, J. Jeslin, and M. L. Verma, "Nanocarriers for drug delivery applications," *Environ. Chem. Lett.* 2019, DOI: 10.1007/s10311-018-00841-1.
- [9] D. Chenthamara, S. Subramaniam, S.G. Ramakrishnan, S. Krishnaswamy, M.M. Essa, F.H. Lin, and M.W. Qoronfleh, "Therapeutic efficacy of nanoparticles and routes of administration," *Biomater. Res.* 2019, DOI: 10.1186/s40824-019-0166-x.
- [10] C. Zhang, L. Yan, X. Wang, S. Zhu, C. Chen, Z. Gu, and Y. Zhao, "Progress, challenges, and future of nanomedicine," *Nano Today* 2020, DOI: 10.1016/j.nantod.2020.101008.
- [11] C. Vauthier and G. Ponchel, Eds., "Polymer nanoparticles for nanomedicines," *Cham: Springer International Publishing* 2016. DOI: 10.1007/978-3-319-41421-8.
- [12] X.Y. Lu, D.C. Wu, Z.J. Li, and G.Q. Chen, "Polymer Nanoparticles," *Prog. Mol Biol. Transl.* 2011, DOI: 10.1016/B978-0-12-416020-0.00007-3.
- [13] R. Mout, D. F. Moyano, S. Rana, and V. M. Rotello, "Surface functionalization of nanoparticles for nanomedicine," *Chem. Soc. Rev.* 2012, DOI: 10.1039/c2cs15294k.
- [14] P. Huang, C. Wang, H. Deng, Y. Zhou, and X. Chen, "Surface engineering of nanoparticles toward cancer theranostics," *Acc. Chem. Res.* 2023, DOI: 10.1021/acs.accounts.3c00122.
- [15] D. Liu, F. Yang, F. Xiong, and N. Gu, "The smart drug delivery system and its clinical potential," *Theranostics* 2016, DOI: 10.7150/thno.14858.
- [16] Y. Liu, G. Yang, S. Jin, L. Xu, and C. Zhao, "Development of high-drug-loading nanoparticles," *Chempluschem* 2020, DOI: 10.1002/cplu.202000496.
- [17] K. C. de Castro, J. M. Costa, and M. G. N. Campos, "Drug-loaded polymeric nanoparticles: a review," *Int. J. Polym. Mater.* 2022, DOI: 10.1080/00914037.2020.1798436.

- [18] C. J. Martínez, M. Tarhini, W. Badri, K. Miladi, H. Greige-Gerges, Q.A. Nazari, S.A.G. Rodríguez, R.A. Román, H. Fessi and A. Elaissari, “Nanoprecipitation process: From encapsulation to drug delivery,” *Int. J. Pharm.* 2017, DOI: 10.1016/j.ijpharm.2017.08.064.
- [19] M. Iqbal, N. Zafar, H. Fessi, and A. Elaissari, “Double emulsion solvent evaporation techniques used for drug encapsulation,” *Int. J. Pharm.* 2015, DOI: 10.1016/j.ijpharm.2015.10.057.
- [20] I. Ekladios, Y. L. Colson, and M. W. Grinstaff, “Polymer–drug conjugate therapeutics: advances, insights and prospects,” *Nat. Rev. Drug. Discov.* 2019, DOI: 10.1038/s41573-018-0005-0.
- [21] F. Seidi, R. Jenjob, and D. Crespy, “Designing smart polymer conjugates for controlled release of payloads,” *Chem. Rev.* 2018, DOI: 10.1021/acs.chemrev.8b00006.
- [22] M. Chang, F. Zhang, T. Wei, T. Zuo, Y. Guan, G. Lin, and W. Shao, “Smart linkers in polymer–drug conjugates for tumor-targeted delivery,” *J. Drug. Target.* 2016, DOI: 10.3109/1061186X.2015.1108324.
- [23] A. V. Kabanov and S. V. Vinogradov, “Nanogels as pharmaceutical carriers: finite networks of infinite capabilities,” *Angew. Chem., Int. Ed. Engl.* 2009, DOI: 10.1002/anie.200900441.
- [24] R. T. Chacko, J. Ventura, J. Zhuang, and S. Thayumanavan, “Polymer nanogels: a versatile nanoscopic drug delivery platform,” *Adv. Drug. Deliv. Rev.* 2012, DOI: 10.1016/j.addr.2012.02.002.
- [25] I. Neamtu, A. G. Rusu, A. Diaconu, L. E. Nita, and A. P. Chiriac, “Basic concepts and recent advances in nanogels as carriers for medical applications,” *Drug Deliv.* 2017, DOI: 10.1080/10717544.2016.1276232.
- [26] K. Narayanan, R. Bhaskar, and S. Han, “Recent advances in the biomedical applications of functionalized nanogels,” *Pharmaceutics* 2022, DOI: 10.3390/pharmaceutics14122832.
- [27] N. K. Preman, S. Jain, and R. P. Johnson, “Smart polymer nanogels as pharmaceutical carriers: a versatile platform for programmed delivery and diagnostics,” *ACS Omega* 2021, DOI: 10.1021/acsomega.0c05276.
- [28] F. Pinelli, M. Saadati, E. N. Zare, P. Makvandi, M. Masi, A. Sacchetti, and F. Rossi, “A perspective on the applications of functionalized nanogels: promises and challenges,” *Int. Mater. Rev.* 2023, DOI: 10.1080/09506608.2022.2026864.
- [29] V. Manimaran, R. P. Nivetha, T. Tamilanban, J. Narayanan, S. Vetrivelan, N. K. Fuloria, S. V. Chinni, M. Sekar, S. Fuloria, L. S. Wong, A. Biswas, G. Ramachawolran, and S. Selvaraj, “Nanogels as novel drug nanocarriers for CNS drug delivery,” *Front. Mol. Biosci.* 2023, DOI: 10.3389/fmolb.2023.1232109.
- [30] Y. Zhang, Z. Zou, S. Liu, S. Miao, and H. Liu, “Nanogels as novel nanocarrier systems for efficient delivery of CNS therapeutics,” *Front. Bioeng. Biotechnol.* 2022, DOI: 10.3389/fbioe.2022.954470.
- [31] M. Suhail, J. M. Rosenholm, M. U. Minhas, S. F. Badshah, A. Naeem, K. U. Khan, and M. Fahad, “Nanogels as drug-delivery systems: a comprehensive overview,” *Ther. Deliv.* 2019, DOI: 10.4155/tde-2019-0010.

- [32] S. V. Vinogradov, E. V. Batrakova, and A. V. Kabanov, "Nanogels for oligonucleotide delivery to the brain," *Bioconjug. Chem.* 2004, DOI: 10.1021/bc034164r.
- [33] L. Ribovski, N. M. Hamelmann, and J. M. J. Paulusse, "Polymeric nanoparticles properties and brain delivery," *Pharmaceutics* 2021, DOI: 10.3390/pharmaceutics13122045.
- [34] A. Azadi, M. R. Rouini, and M. Hamidi, "Neuropharmacokinetic evaluation of methotrexate-loaded chitosan nanogels," *Int. J. Biol. Macromol.* 2015, DOI: 10.1016/j.ijbiomac.2015.05.001.
- [35] A. B. Richard, S. Krakowka, L. B. Dexter, H. Schmid, A. P. M. Wolterbeek, D. H. Waalkens-Berendsen, and M. Kurimoto, "Trehalose: a review of properties, history of use and human tolerance, and results of multiple safety studies," *Food Chem. Toxicol.* 2002, DOI: 10.1016/S0278-6915(02)00011-X.
- [36] S. Ohtake and Y. J. Wang, "Trehalose: current use and future applications," *J. Pharm. Sci.* 2011, DOI: 10.1002/jps.22458.
- [37] Y. H. Kim, T. K. Kwon, S. Park, H. S. Seo, J. J. Cheong, C. H. Kim, J. S. Lee, and Y. D. Choi, "Trehalose synthesis by sequential reactions of recombinant maltooligosyltrehalose synthase and maltooligosyltrehalose trehalohydrolase from *brevibacterium helvolum*," *Appl. Environ. Microbiol.* 2000, DOI: 10.1128/AEM.66.11.4620-4624.2000.
- [38] D. Kuczyńska-Wiśnik, K. Stojowska-Swędryńska, and E. Laskowska, "Intracellular Protective Functions and Therapeutical Potential of Trehalose," *Molecules* 2024, DOI: 10.3390/molecules29092088.
- [39] P. Mardones, D. C. Rubinsztein, and C. Hetz, "Mystery solved: trehalose kickstarts autophagy by blocking glucose transport," *Sci. Signal.* 2016, DOI: 10.1126/scisignal.aaf1937.
- [40] K. Hosseinpour-Moghaddam, M. Caraglia, and A. Sahebkar, "Autophagy induction by trehalose: molecular mechanisms and therapeutic impacts," *J. Cell. Physiol.* 2018, DOI: 10.1002/jcp.26583.
- [41] A. B. Pupyshev, T. P. Klyushnik, A. A. Akopyan, S. K. Singh, and M. A. Tikhonova, "Disaccharide trehalose in experimental therapies for neurodegenerative disorders: Molecular targets and translational potential," *Pharmacol. Res.* 2022, DOI: 10.1016/j.phrs.2022.106373.
- [42] D. J. Klionsky, G. Petroni, R. K. Amaravadi et al., "Autophagy in major human diseases," *EMBO J.* 2021, DOI: 10.15252/embj.2021108863.
- [43] M. Kitada and D. Koya, "Autophagy in metabolic disease and ageing," *Nat. Rev. Endocrinol.* 2021, DOI: 10.1038/s41574-021-00551-9.
- [44] B. J. DeBosch, M. R. Heitmeier, A. Mayer, C. B. Higgins, J. R. Crowley, T. E. Kraft, M. Chi, E. P. Newberry, Z. Chen, B. N. Finck, N. O. Davidson, K. E. Yarasheski, P. W. Hruz, and K. H. Moley, "Trehalose inhibits solute carrier 2A (SLC2A) proteins to induce autophagy and prevent hepatic steatosis," *Sci. Signal.* 2016, DOI: 10.1126/scisignal.aac5472.
- [45] A. L. Mayer, C. B. Higgins, M. R. Heitmeier, T. E. Kraft, X. Qian, J. R. Crowley, K. L. Hyrc, W. L. Beatty, K. E. Yarasheski, P. W. Hruz, and B. J. DeBosch, "SLC2A8 (GLUT8) is a mammalian trehalose transporter required for trehalose-induced autophagy," *Sci. Rep.* 2016, DOI: 10.1038/srep38586.

- [46] P. Rusmini, K. Cortese, V. Crippa et al., “Trehalose induces autophagy via lysosomal-mediated TFEB activation in models of motoneuron degeneration,” *Autophagy* 2019, DOI: 10.1080/15548627.2018.1535292.
- [47]* [P1] A. Maruf, M. Milewska, M. Varga, and I. Wandzik, “Trehalose-bearing carriers to target impaired autophagy and protein aggregation diseases,” *J. Med. Chem.* 2023, DOI: 10.1021/acs.jmedchem.3c01442.
- [48] J. Collins, C. Robinson, H. Danhof, C. W. Knetsch, H. C. van Leeuwen, T. D. Lawley, J. M. Auchtung, and R. A. Britton, “Dietary trehalose enhances virulence of epidemic *Clostridium difficile*,” *Nature* 2018, DOI: 10.1038/nature25178.
- [49] Z. Li, L. Zhang, C. Xue, Y. Zhang, Y., Yu, X. Guo, and Z. Zhang, “Hydroxypropyl- β -cyclodextrin/oridonin and trehalose loaded nanovesicles attenuate foam cells formation and regulate the inflammation,” *Eur. Polym. J.* 2022, DOI: 10.1016/j.eurpolymj.2022.111596.
- [50] J. Yang, L. Ding, L. Yu, Y. Wang, M. Ge, Q. Jiang, and Y. Chen, “Nanomedicine enables autophagy-enhanced cancer-cell ferroptosis,” *Sci. Bull.* 2021, DOI: 10.1016/j.scib.2020.10.021.
- [51] G. Frapporti, E. Colombo, H. Ahmed, G. Assoni, L. Polito, P. Randazzo, D. Arosio, P. Seneci, and G. Piccoli, “Squalene-based nano-assemblies improve the pro-autophagic activity of trehalose,” *Pharmaceutics* 2022, DOI: 10.3390/pharmaceutics14040862.
- [52] Z. Wu, M. Zhou, X. Tang, J. Zeng, Y. Li, Y. Sun, J. Huang, L. Chen, M. Wan, and C. Mao, “Carrier-free trehalose-based nanomotors targeting macrophages in inflammatory plaque for treatment of atherosclerosis,” *ACS Nano* 2022, DOI: 10.1021/acsnano.1c08391.
- [53] A. Cunha, A. Gaubert, J. Verget, M. L. Thiolat, P. Barthélémy, L. Latxague, and B. Dehay, “Trehalose-based nucleolipids as nanocarriers for autophagy modulation: an in vitro study,” *Pharmaceutics* 2022, DOI: 10.3390/pharmaceutics14040857.
- [54] E. Colombo, M. Biocotino, G. Frapporti, P. Randazzo, M. S. Christodoulou, G. Piccoli, L. Polito, P. Seneci, and D. Passarella, “Nanolipid-trehalose conjugates and nano-assemblies as putative autophagy inducers,” *Pharmaceutics* 2019, DOI: 10.3390/pharmaceutics11080422.
- [55] G. Assoni, G. Frapporti, E. Colombo, D. Gornati, M. D. Perez-Carrion, L. Polito, P. Seneci, G. Piccoli, and D. Arosio, “Trehalose-based neuroprotective autophagy inducers,” *Bioorg. Med. Chem. Lett.* 2021, DOI: 10.1016/j.bmcl.2021.127929.
- [56] C. B. Higgins, J. A. Adams, M. H. Ward, Z. J. Greenberg, M. Milewska, J. Sun, Y. Zhang, P.L. Chiquetto Q. Dong, S. Ballentine, W. Li, I. Wandzik, L. G. Schuettpelez, and B. J. DeBosch, “The tetraspanin transmembrane protein CD53 mediates dyslipidemia and integrates inflammatory and metabolic signaling in hepatocytes,” *J. Bio. Chem.* 2023, DOI: 10.1016/j.jbc.2022.102835.
- [57]* [P2] A. Maruf, M. Milewska, A. Lalik, and I. Wandzik, “pH and reduction dual-responsive nanogels as smart nanocarriers to resist doxorubicin aggregation,” *Molecules* 2022, DOI: 10.3390/molecules27185983.
- [58]* [P3] A. Maruf, M. Milewska, A. Lalik, S. Student, and I. Wandzik, “A simple synthesis of reduction-responsive acrylamide-type nanogels for miRNA delivery,” *Molecules* 2023, DOI: 10.3390/molecules28020761.

- [59]* [P4] A. Maruf, M. Milewska, T. Kovács, M. Varga, T. Vellai, A. Lalik, S. Student, O. Borges, and I. Wandzik, “Trehalose-releasing nanogels: A step toward a trehalose delivery vehicle for autophagy stimulation,” *Biomater. Adv.* 2022, DOI: 10.1016/j.bioadv.2022.212969.
- [60]* [P5] Y. Zhong, A. Maruf, K. Qu, M. Milewska, I. Wandzik, N. Mou, Y. Cao, and W. Wu, “Nanogels with covalently bound and releasable trehalose for autophagy stimulation in atherosclerosis,” *J. Nanobiotechnol.* 2023, DOI: 10.1186/s12951-023-02248-9.
- [61] K. Landfester, “Polyreactions in miniemulsions,” *Macromol. Rapid. Commun.* 2001, DOI: 10.1002/1521-3927(20010801)22:12<896::AID-MARC896>3.0.CO;2-R.
- [62] J. M. Asua, “Miniemulsion polymerization,” in *Encyclopedia of Polymeric Nanomaterials, Berlin, Heidelberg: Springer Berlin Heidelberg* 2015, DOI: 10.1007/978-3-642-29648-2_263.
- [63] J. M. Asua, “Miniemulsion polymerization,” *Prog. Polym. Sci.* 2002, DOI: 10.1016/S0079-6700(02)00010-2.
- [64] U. Kanwal, N. Irfan Bukhari, M. Ovais, N. Abass, K. Hussain, and A. Raza, “Advances in nano-delivery systems for doxorubicin: an updated insight,” *J. Drug. Target.* 2018, DOI: 10.1080/1061186X.2017.1380655.
- [65] R. Cheng, F. Feng, F. Meng, C. Deng, J. Feijen, and Z. Zhong, “Glutathione-responsive nano-vehicles as a promising platform for targeted intracellular drug and gene delivery,” *J. Control. Release* 2011, DOI: 10.1016/j.jconrel.2011.01.030.
- [66] G. Hao, Z. P. Xu, and L. Li, “Manipulating extracellular tumour pH: an effective target for cancer therapy,” *RSC Adv.* 2018, DOI: 10.1039/C8RA02095G.
- [67] Y. Peng and C. M. Croce, “The role of microRNAs in human cancer,” *Signal. Transduct. Target. Ther.* 2016, DOI: 10.1038/sigtrans.2015.4.
- [68] H. W. Hwang and J. T. Mendell, “MicroRNAs in cell proliferation, cell death, and tumorigenesis,” *Br. J. Cancer.* 2006, DOI: 10.1038/sj.bjc.6603023.
- [69] V. Baumann and J. Winkler, “miRNA-based therapies: strategies and delivery platforms for oligonucleotide and non-oligonucleotide agents,” *Future Med. Chem.* 2014, DOI: 10.4155/fmc.14.116.
- [70] F. Seidi, R. Jenjob, and D. Crespy, “Designing smart polymer conjugates for controlled release of payloads,” *Chem. Rev.* 2018, DOI: 10.1021/acs.chemrev.8b00006.
- [71] C. P. McCoy, R. J. Morrow, C. R. Edwards, D. S. Jones, and S. P. Gorman, “Neighboring group-controlled hydrolysis: towards ‘designer’ drug release biomaterials,” *Bioconjug. Chem.* 2007, DOI: 10.1021/bc060238y.
- [72] M. Burek, S. Waśkiewicz, A. Lalik, and I. Wandzik, “Hydrogels with novel hydrolytically labile trehalose-based crosslinks: small changes – big differences in degradation behavior,” *Polym. Chem.* 2018, DOI: 10.1039/C8PY00488A.
- [73] M. Burek and I. Wandzik, “Trehalose-rich, degradable hydrogels designed for trehalose release under physiologically relevant conditions,” *Polymers* 2019, DOI: 10.3390/polym11122027.
- [74] C. F. Bennett, A. R. Krainer, and D. W. Cleveland, “Antisense oligonucleotide therapies for neurodegenerative diseases,” *Annu. Rev. Neurosci.* 2019, DOI: 10.1146/annurev-neuro-070918-050501.

- [75] A. Vashist, A. Kaushik, A. Vashist, J. Bala, R. Nikkhah-Moshaie, V. Sagar, and M. Nair, "Nanogels as potential drug nanocarriers for CNS drug delivery," *Drug Discov. Today* 2018, DOI: 10.1016/j.drudis.2018.05.018.
- [76] N. Lewinski, V. Colvin, and R. Drezek, "Cytotoxicity of Nanoparticles," *Small* 2008, DOI: 10.1002/sml.200700595.
- [77] M. Awashra and P. Młynarz, "The toxicity of nanoparticles and their interaction with cells: an in vitro metabolomic perspective," *Nanoscale Adv.* 2023, DOI: 10.1039/D2NA00534D.
- [78] T. L. Moore, L. Rodriguez-Lorenzo, V. Hirsch, S. Balog, D. Urban, C. Jud, B. Rothen-Rutishauser, M. Lattuada, and A. Petri-Fink, "Nanoparticle colloidal stability in cell culture media and impact on cellular interactions," *Chem. Soc. Rev.* 2015, DOI: 10.1039/c4cs00487f.
- [79] A. Sizovs, L. Xue, Z. P. Tolstyka, N. P. Ingle, Y. Wu, M. Cortez, and T. M. Reineke, "Poly(trehalose): sugar-coated nanocomplexes promote stabilization and effective polyplex-mediated siRNA delivery," *J. Am. Chem. Soc.* 2013, DOI: 10.1021/ja404941p.
- [80] S. Srinivasachari, Y. Liu, L. E. Pevette, and T. M. Reineke, "Effects of trehalose click polymer length on pDNA complex stability and delivery efficacy," *Biomaterials* 2007, DOI: 10.1016/j.biomaterials.2007.01.037.
- [81] K. M. Meek, J. R. Nykaza, and Y. A. Elabd, "Alkaline chemical stability and ion transport in polymerized ionic liquids with various backbones and cations," *Macromolecules* 2016, DOI: 10.1021/acs.macromol.6b00434.
- [82] F. C. Baines and J. C. Bevington, "A tracer study of the hydrolysis of methyl methacrylate and methyl acrylate units in homopolymers and copolymers," *J. Polym. Sci.* 1968, DOI: 10.1002/pol.1968.150060901.
- [83] Y. S. Jo, J. Gantz, J. A. Hubbell, and M. P. Lutolf, "Tailoring hydrogel degradation and drug release via neighboring amino acid controlled esterhydrolysis," *Soft Matter* 2009, DOI: 10.1039/B814584A.
- [84] C. Mauvezin, C. Ayala, C. R. Braden, J. Kim, and T. P. Neufeld, "Assays to monitor autophagy in *Drosophila*," *Methods* 2014, DOI: 10.1016/j.ymeth.2014.03.014.
- [85] E. Blanco, H. Shen, and M. Ferrari, "Principles of nanoparticle design for overcoming biological barriers to drug delivery," *Nat. Biotechnol.* 2015, DOI: 10.1038/nbt.3330.
- [86] F. Alexis, E. Pridgen, L. K. Molnar, and O. C. Farokhzad, "Factors affecting the clearance and biodistribution of polymeric nanoparticles," *Mol. Pharm.* 2008, DOI: 10.1021/mp800051m.
- [87] F. Veider, E. Sanchez Armengol, and A. Bernkop-Schnürch, "Charge-reversible nanoparticles: advanced delivery systems for therapy and diagnosis," *Small* 2024, DOI: 10.1002/sml.202304713.
- [88] H. Chen, Q. Hu, W. Li, X. Cai, L. Mao, and R. Li, "Approaches to nanoparticle labeling: a review of fluorescent, radiological, and metallic techniques," *Environ. Health* 2023, DOI: 10.1021/envhealth.3c00034.
- [89] F. Le Guern, V. Mussard, A. Gaucher, M. Rottman, and D. Prim, "Fluorescein derivatives as fluorescent probes for pH monitoring along recent biological applications," *Int. J. Mol. Sci.* 2020, DOI: 10.3390/ijms21239217.

- [90] D. P. Surzhikova, L. A. Sukovatyi, E. V. Nemtseva, E. N. Esimbekova, and E. A. Slyusareva, "Functioning of a fluorescein pH-probe in aqueous media: impact of temperature and viscosity," *Micromachines* 2023, DOI: 10.3390/mi14071442.

6. Academic achievements

Academic achievements related to doctoral dissertation

Publications:

1. [P1] Maruf A*, Milewska M*, Varga M, Wandzik I*. *Trehalose-Bearing Carriers to Target Impaired Autophagy and Protein Aggregation Diseases*. **J. Med. Chem.** 2023, 66, 15613–15628. DOI: 10.1021/acs.jmedchem.3c01442.
(IF₂₀₂₂ = 7.300, MEiN = 200 point, *contributed equally)
2. [P2] Maruf A, Milewska M, Lalik A, Wandzik I. *pH and Reduction Dual-Responsive Nanogels as Smart Nanocarriers to Resist Doxorubicin Aggregation*. **Molecules**. 2022, 27, 5983. DOI: 10.3390/molecules27185983.
(IF₂₀₂₁ = 4.927, MEiN = 140 point)
3. [P3] Maruf A, Milewska M, Lalik A, Student S, Wandzik I. *A Simple Synthesis of Reduction-Responsive Acrylamide-Type Nanogels for miRNA Delivery*. **Molecules**. 2023, 28, 761. DOI: 10.3390/molecules28020761.
(IF₂₀₂₂ = 4.600, MEiN = 140 point)
4. [P4] Maruf A, Milewska M, Kovács T, Varga M, Vellai T, Lalik A, Student S, Borges O, Wandzik I. *Trehalose-releasing nanogels: A step toward a trehalose delivery vehicle for autophagy stimulation*. **Biomater. Adv.** 2022, 138, 212969. DOI: 10.1016/j.bioadv.2022.212969.
(formerly known as **Mater. Sci. Eng. C** with IF₂₀₂₁ = 7.328, MEiN = 140 point)
5. [P5] Zhong Y*, Maruf A*, Qu K, Milewska M, Wandzik I, Mou N, Cao Y, Wu W. *Nanogels with covalently bound and releasable trehalose for autophagy stimulation in atherosclerosis*. **J. Nanobiotechnol.** 2023, 21, 472. DOI: 10.1186/s12951-023-02248-9.
(IF₂₀₂₂ = 10.200, MEiN = 140 point, *contributed equally)

Conferences:

1. Maruf A, Milewska M, Salvati A, Wandzik I. The surface charge effects of trehalose-releasing nanogels on trehalose release, protein corona formation, and cell uptake. Oral presentation at Pharmacy Day 2024, The University of Groningen. 11 June 2024, Groningen, The Netherlands.
2. Maruf A, Milewska M, Wandzik I. Synthesis and characterization of trehalose-containing nanocarriers for potential cancer treatments. Poster presentation at the 27th Gliwice Scientific Meetings. 16-17 November 2023, Gliwice, Poland.

3. Maruf A, Lalik A, Milewska M, Wandzik I. Nanoparticles as intracellular trehalose delivery systems for cryopreservation. Poster presentation at the 12th International Colloids Conference (Elsevier). 11-14 June 2023, Palma, Spain.
4. Maruf A, Lalik A, Milewska M, Wandzik I. Polymers releasing trehalose as a potential solvent-free cell banking. Oral presentation at Computational Oncology and Personalized Medicine – Crossing Borders, Connecting Science (COPM2023) Conference. 26th April 2023, Gliwice, Poland.
5. Maruf A, Milewska M, Lalik A, Wandzik I. Smart pH/redox dual-responsive nanogels as doxorubicin delivery systems. Poster presentation at the 26th Gliwice Scientific Meetings. 18-19 November 2022, Gliwice, Poland.
6. Maruf A, Milewska M, Lalik A, Wandzik I. Glutathione-responsive nanogels as drug delivery systems. Oral presentation at NanoTech Poland 2022. 1-3 June 2022, Poznan, Poland.
7. Maruf A, Milewska M, Lalik A, Student S, Wandzik I. Trehalose-releasing nanogels: a potential trehalose delivery system for autophagy stimulation. Oral presentation at the 25th Anniversary of Gliwice Scientific Meetings: Joint online seminar of the Polish Proteomics Society and the Finnish Proteomics Society: Proteomics of Extracellular Vesicles. 18-20 November 2021, Gliwice, Poland.
8. Milewska M, Maruf A, Waśkiewicz S, Lalik A, Student S, Wandzik I. Micro- and nanosized hydrogels for biomedical applications. Co-author of the short lecture by Prof. Ilona Wandzik at the 25th Anniversary of Gliwice Scientific Meetings: Joint online seminar of the Polish Proteomics Society and the Finnish Proteomics Society: Proteomics of Extracellular Vesicles. 18-20 November 2021, Gliwice, Poland.
9. Maruf A, Milewska M, Lalik A, Student S, Wandzik I. A Series of Trehalose-Releasing Polymers as Potential Drug Delivery Agents for Autophagy Stimulation. Poster presentation at the 7th Young Polymer Scientists Conference and Short Course. 27-28 September 2021, Lodz, Poland.

Project:

Title of project: Trehalose releasing nanogels for autophagy stimulation (PRELUDIUM BIS 1, Grant No. 2019/35/O/ST5/02746, The National Science Center (NCN), Poland)

Project duration: 01/10/2020 to 30/09/2024 (48 months)

The function performed in the project: main contractor (project manager: prof. dr hab. inż. Ilona Wandzik)

Patent application:

Ilona Wandzik, Małgorzata Milewska, Ali Maruf; Sposób otrzymywania nanożeli uwalniających kowalencyjnie związaną trehalozę.

Patent application number: P.438753 , submission date: 16 August 2021, Urząd Patentowy RP, Warszawa, Poland.

Awards:

Pro-quality scholarship for the best PhD students of The Silesian University of Technology in four academic years (2020/2021, 2021/2022, 2022/2023, and 2023/2024), under the implementation of The Excellence Initiative – Research University (IDUB, 2020–2026) program (08/IDUB/2019/94)

Foreign internships:

1. Research Internship at The University of Helsinki, Finland; Duration: 6 months, from 01.02.2023 to 01.08.2023; Foreign supervisor: Prof. Mikko Airavaara; Research activities: conducting research on trehalose-releasing nanogel effects on *in vivo* model of Parkinson's Diseases as part of Project PRELUDIUM BIS 1 (2019/35/O/ST5/02746) from NCN, Poland; The mobility was funded by NAWA (PPN/STA/2021/1/00053), external grant.
2. Research Internship at The University of Coimbra, Portugal; Duration: 2 weeks, from 05.09.2021 to 15.09.2021; Foreign supervisor: Dr. Olga Borges; Research activities: conducting research on investigation of the hemolysis property of trehalose-releasing nanogels on human red blood cells as part of Project PRELUDIUM BIS 1 (2019/35/O/ST5/02746) from NCN, Poland; The mobility was funded by NAWA under PROM program (POWR.03.03.00-IP.08-00-P13/18), managed by The Silesian University of Technology.
3. Research Internship at The University of Groningen, the Netherlands; Duration: 3 months, from 02.04.2024 to 28.06.2024; Foreign supervisor: Prof. Anna Salvati; Research activities: conducting research on investigation of the effects of cationic, anionic, and zwitterionic trehalose-releasing nanogels on protein corona formation and uptake mechanisms as part of Project PRELUDIUM BIS 1 (2019/35/O/ST5/02746) from NCN, Poland; The mobility was funded by The Silesian University of Technology through the mobility scholarships for the best PhD students of The Silesian University of Technology (2023/2024 academic year, Decision no. RJO15.5033.455.2023) under the implementation of The Excellence Initiative

– Research University (IDUB, 2020–2026) program (08/IDUB/2019/94) co-financed with the PRELUDIUM BIS 1 project (2019/35/O/ST5/02746).

Peer review experience:

1. Heliyon (Cell Press, IF₂₀₂₂ = 4.000)

Reviewing 4 submitted manuscripts. Source-Work-ID: 8a0f0857-c2c7-457a-890a-cc4c3a61fe3b; e4b0d526-9e8c-46e3-9ced-7b4f3814b54c; 74ef6e7eebfd-4c8c-ae55-4614bc24a742; and e35ec29b-db0f-4c59-9bc7-6c64f21983ff.

2. Pharmaceutics (MDPI, IF₂₀₂₂: 5.400)

Reviewing 3 submitted manuscripts. Source-Work-ID: 25918417; 25916096; and 25641333.

3. Biosensors (MDPI, IF₂₀₂₂: 5.400)

Reviewing 1 submitted manuscript. Source-Work-ID: 24610287.

Note: peer review experience are all recorded in ORCID: 0000-0003-3807-4446.

Academic achievements not related to doctoral dissertation

Publications:

1. Pujimulyani D, Yulianto WA, Setyowati A, Prastyo P, Windrayahya S, Maruf A. White saffron (*Curcuma mangga Val.*) attenuates diabetes and improves pancreatic β -cell regeneration in streptozotocin-induced diabetic rats. **Toxicol. Rep.** 2022, 9, 1213–1221. DOI: 10.1016/j.toxrep.2022.05.014. (Citescore₂₀₂₂ = 7.200)
2. Wang Y, Zhang K, Li T, Maruf A, Qin X, Luo L, Zhong Y, Qiu J, McGinty S, Pontrelli G, Liao X, Wu W, Wang G. Macrophage membrane functionalized biomimetic nanoparticles for targeted anti-atherosclerosis applications. **Theranostics** 2021, 11, 164–180. DOI: 10.7150/thno.47841. (IF₂₀₂₂ = 12.400)
3. Liu B, Yan W, Luo L, Wu S, Wang Y, Zhong Y, Tang D, Maruf A, Yan M, Zhang K, Qin X, Qu K, Wu W, Wang G. Macrophage membrane camouflaged reactive oxygen species responsive nanomedicine for efficiently inhibiting the vascular intimal hyperplasia. **J. Nanobiotechnol.** 2021, 19, 374. DOI: 10.1186/s12951-021-01119-5. (IF₂₀₂₂ = 10.200)

4. Rumanti AP, Maruf A, Liu H, Ge S, Lei D, Wang G. *Engineered bioresponsive nanotherapeutics: recent advances in the treatment of atherosclerosis and ischemic-related disease*. **J. Mater. Chem. B** 2021, 9, 4804–4825. DOI: 10.1039/d1tb00330e.
(IF₂₀₂₂ = 7.000)
5. Tang D, Wang Y, Wijaya A, Liu B, Maruf A, Wang J, Xu J, Liao X, Wu W, Wang G. *ROS-responsive biomimetic nanoparticles for potential application in targeted anti-atherosclerosis*. **Regen. Biomater.** 2021, 8, rbab033. DOI: 10.1093/rb/rbab033.
(IF₂₀₂₂ = 6.700)
6. Gafur A, Sukamdani GY, Kristi N, Maruf A, Xu J, Chen X, Wang G, Ye Z. *From bulk to nano-delivery of essential phytochemicals: recent progress and strategies for antibacterial resistance*. **J. Mater. Chem. B** 2020, 8, 9825–9835. DOI: 10.1039/d0tb01671c.
(IF₂₀₂₂ = 7.000)
7. Wijaya A, Maruf A, Wu W, Wang G. *Recent advances in micro- and nano-bubbles for atherosclerosis applications*. **Biomater. Sci.** 2020, 8, 4920–4939. DOI: 10.1039/d0bm00762e.
(IF₂₀₂₂ = 6.600)
8. Maruf A, Wang Y, Luo L, Zhong Y, Nurhidayah D, Liu B, Rouf MA, Zhang H, Yin, Y, Wu W., Wang G. *Nanoerythrocyte Membrane-Enveloped ROS-Responsive 5-Aminolevulinic Acid Prodrug Nanostructures with Robust Atheroprotection*. **Part. Part. Sys. Char.** 2020, 37, 2000021. DOI: 10.1002/ppsc.202000021.
(IF₂₀₂₂ = 2.700)
9. Pujimulyani D, Suryani CL, Setyowati A, Handayani RAS, Arumwardana S, Widowati W, Maruf A. *Cosmeceutical potentials of Curcuma mangga Val. extract in human BJ fibroblasts against MMP1, MMP3, and MMP13*. **Heliyon** 2020, 6, e04921. DOI: 10.1016/j.heliyon.2020.e04921.
(IF₂₀₂₂ = 4.000)
10. Pujimulyani D, Santoso U, Luwihana DS, Maruf A. *Orally administered pressure-blanching white saffron (Curcuma mangga Val.) improves antioxidative properties and lipid profiles in vivo*. **Heliyon** 2020, 6, e04219. DOI: 10.1016/j.heliyon.2020.e04219.
(IF₂₀₂₂ = 4.000)
11. Pujimulyani D, Yulianto WA, Setyowati A, Arumwardana S, Sari Widya Kusuma H, Adhani Sholihah I, Rizal R, Widowati W, Maruf A. *Hypoglycemic Activity of Curcuma mangga Val. Extract via Modulation of GLUT4 and PPAR- γ mRNA Expression in 3T3-L1 Adipocytes*. **J. Exp. Pharmacol.** 2020, 12, 363–369. DOI: 10.2147/JEP.S267912.

(Citescore₂₀₂₂ = 5.400)

12. Maruf A, Wang Y, Yin T, Huang J, Wang N, Durkan C, Tan Y, Wu W, Wang G. *Atherosclerosis Treatment with Stimuli-Responsive Nanoagents: Recent Advances and Future Perspectives*. **Adv. Healthcare Mater.** 2019, 8, e1900036. DOI: 10.1002/adhm.201900036.

(IF₂₀₂₂ = 10.000)

13. Gafur A, Kristi N, Maruf A, Wang G, Ye Z. *Transforming stealthy to sticky nanocarriers: a potential application for tumor therapy*. **Biomater. Sci.** 2019, 7, 3581–3593. DOI: 10.1039/c9bm00724e.

(IF₂₀₂₂ = 6.600)

14. Nurhidayah D, Maruf A, Zhang X, Liao X, Wu W, Wang G. *Advanced drug-delivery systems: mechanoresponsive nanoplatforms applicable in atherosclerosis management*. **Nanomedicine** 2019, 14, 3105–3122. DOI: 10.2217/nnm-2019-0172.

(IF₂₀₂₂ = 5.500)

15. Zhong Y, Wang Y, Luo L, Nurhidayah D, Maruf A, Gregersen H, Wu W, Wang G. *Targeted polyethylenimine/(p53 plasmid) nanocomplexes for potential antitumor applications*. **Nanotechnol.** 2019, 30, 145601. DOI: 10.1088/1361-6528/aaf41a.

(IF₂₀₂₂ = 3.500)

16. Luo L, Wu W, Sun D, Dai H B, Wang Y, Zhong Y, Wang JX, Maruf A, Nurhidayah D, Zhang XJ, Wang Y, Wang GX. *Acid-Activated Melittin for Targeted and Safe Antitumor Therapy*. **Bioconjugate Chem.** 2018, 29(9), 2936–2944. DOI: 10.1021/acs.bioconjchem.8b00352.

(IF₂₀₂₂ = 4.700)

Awards:

Chinese Government Scholarship for Outstanding International Student (2019, National award given to the best 100 international students in China).